Volume 14 | Number 44 | 28 November 2016 | Pages 10315–10536

Organic & Biomolecular Chemistry

www.rsc.org/obc

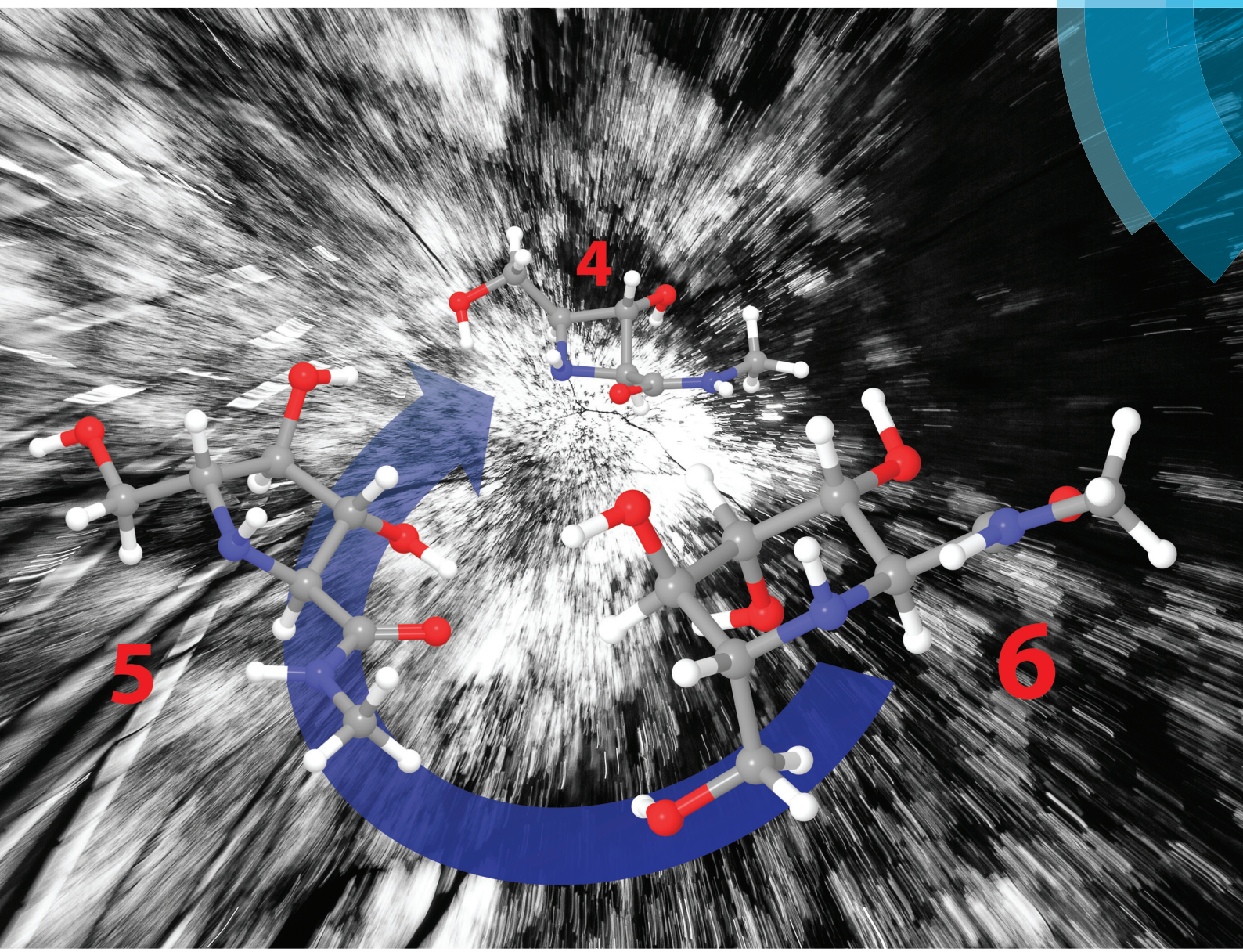

ISSN 1477-0520

ROYAL SOCIETY OF CHEMISTRY

PAPER

A. F. G. Glawar, A. Kato, S. F. Jenkinson *et al.*

Structural essentials for β-*N*-acetylhexosaminidase inhibition by amides of prolines, pipecolic and azetidine carboxylic acids

175 YEARS

Organic & Biomolecular Chemistry

PAPER

View Article Online
View Journal | View Issue

Cite this: *Org. Biomol. Chem.*, 2016, **14**, 10371

Structural essentials for β-*N*-acetylhexosaminidase inhibition by amides of prolines, pipecolic and azetidine carboxylic acids†

A. F. G. Glawar,[a,b] R. F. Martínez,[a] B. J. Ayers,[a] M. A. Hollas,[a] N. Ngo,[a] S. Nakagawa,[c] A. Kato,*[c] T. D. Butters,[b] G. W. J. Fleet[a,b] and S. F. Jenkinson*[a]

Received 20th July 2016,
Accepted 6th October 2016

DOI: 10.1039/c6ob01549b

www.rsc.org/obc

This paper explores the computer modelling aided design and synthesis of β-*N*-acetylhexosaminidase inhibitors along with their applicability to human disease treatment through biological evaluation in both an enzymatic and cellular setting. We investigated the importance of individual stereocenters, variations in structure–activity relationships along with factors influencing cell penetration. To achieve these goals we modified nitrogen heterocycles in terms of ring size, side chains present and ring nitrogen derivatization. By reducing the inhibitor interactions with the active site down to the essentials we were able to determine that besides the established 2*S*,3*R* *trans*-relationship, the presence and stereochemistry of the CH_2OH side chain is of crucial importance for activity. In terms of cellular penetration, *N*-butyl side chains favour cellar uptake, while hydroxy- and carboxy-group bearing sidechains on the ring nitrogen retarded cellular penetration. Furthermore we show an early proof of principle study that β-*N*-acetylhexosaminidase inhibitors can be applicable to use in a potential anti-invasive anti-cancer strategy.

Introduction

Glycoproteins and glycosphingolipids (GSLs) are ubiquitous components of eukaryotic cell membranes where they contribute both to structural integrity and the recognition and signalling between cells and binding partners in the extracellular space.[1] The covalently bound oligosaccharide linked to asparagine or serine and threonine residues in glycoproteins contains *N*-acetylglucosamine (GlcNAc) and *N*-acetylgalactosamine (GalNAc) as the terminal reducing sugar in *N*-linked and *O*-linked glycoproteins, respectively, and as part of the extended glycan chain. GSLs also contain these *N*-acetylhexosamine (HexNAc) residues at non-reducing positions in the glycan chain.

Lysosomal catabolism of glycoproteins and GSLs is an essential part in the maintenance of cell surface membranes and deficiencies in HexNAcase activity are responsible for genetically inherited storage disorders in man, including Tay-Sachs, Sandhoff and Schindler-Kanzaki disease.[2] There are few therapeutic options for treating these disorders, but the design of enzyme-targeted inhibitors, or carbohydrate mimics such as iminosugars that act as chaperones, offers a potential route for enhancing enzyme activity in the lysosome (Fig. 1).[3]

Pyrrolidine iminosugar *O*-GlcNAcase (OGA) inhibitors may be useful in the study of Alzheimer's disease.[4] Crystallographic studies of OGA have given insight into the active site of this class of enzyme;[5] recent studies have probed the transition state binding interactions of aminothiazoline inhibitors of *O*-GlcNacase.[4b]

HexNAcase is also one of the glycosidases secreted into extra cellular space by cancer cells in the cocktail of enzymes to remodel and degrade the extra cellular matrix (ECM), allowing the cancer to spread to secondary locations in a process known as metastasis formation.[6] Although the inhibition of proteases to prevent metastasis formation is well established, the use of iminosugars to inhibit glycosidases like HexNAcase has been less commonly employed.[7] Many components of the ECM however contain carbohydrate residues and hence inhibition of HexNAcase is a viable anti-invasive strategy.

Nanomolar iminosugar inhibitors of HexNAcases (Fig. 1) have been isolated from bacterial broths including: siastatin B **1**,[8] pochonicine **2**[9] and nagstatin **3**.[10] HexNAcase inhibitors containing an acetamide-group have been synthesised in various ring sizes ranging from 6- to 4-ring (Fig. 1). Featuring a

[a]*Chemistry Research Laboratory, 12 Mansfield Road, Oxford, OX1 3TA, UK. E-mail: sarah.jenkinson@chem.ox.ac.uk; Fax: +44 (0)1865 285002; Tel: +44 (0)1865 275645*
[b]*Oxford Glycobiology Institute, University of Oxford, South Parks Road, Oxford, OX1 3QU, UK. Fax: +44 (0)1865 275216; Tel: +44 (0)1865 275342*
[c]*Department of Hospital Pharmacy, University of Toyama, 2630 Sugitani, Toyama 930-0194, Japan. E-mail: kato@med.u-toyama.ac.jp*
†Electronic supplementary information (ESI) available. See DOI: 10.1039/c6ob01549b

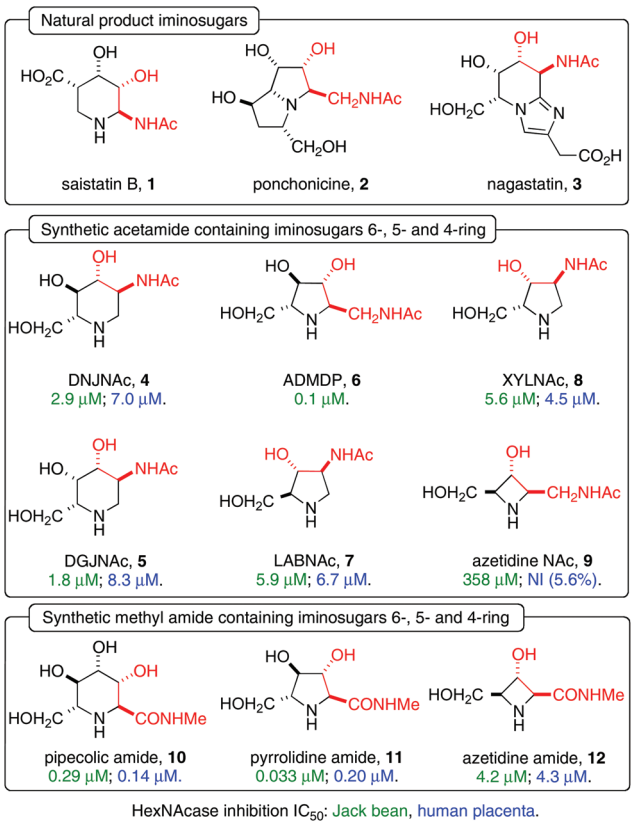

Fig. 1 Potent HexNAcase inhibitors containing acetamide or methyl amide group. Highlighted in red *2S,3R trans*-relationship present in potent inhibitors.

piperidine scaffold this has included DNJNAc **4** [11] and DGJNAc **5**, the latter is also the most powerful inhibitor of the glycosidase α-*N*-acetylgalactosaminidase known to date.[12] Equally several powerful HexNAc inhibitors with a 5-ring scaffold and a NAc group are known. This group incorporates the pyrrolidines devised by Wong *et al.* including ADMDP **6** (0.1 μM, Jack bean),[13] and the 5-carbon scaffold based LABNAc **7** (6.7 μM, human placenta),[14] and XYLNAc **8** (4.5 μM, human placenta).[15] The latter is a very recent addition to the stock of known HexNAc inhibitors along with the 4-ring inhibitor **9** (358 μM) based on the azetidine scaffold.[16]

In previous studies the methyl amide group has been recognized as a bioisostere of the NAc group and inhibitors ranging in ring size from 6 to 4 have also been devised featuring this functional group (Fig. 1). This has included the pipecolic amide **10** [17] containing a piperidine ring, which is a powerful HexNAcase inhibitor (0.14 μM, human placenta) and is the starting point for this study. The 5-ring pyrrolidine amide **11** [16] is equally powerful (0.20 μM, human placenta) and structurally highly related to ADMDP **6**. In terms of the 4-ring system the azetidine amide **12** (4.3 μM, human placenta) has recently been synthesised.[18] The hexosaminidases HexA and HexB from human placenta have been crystallised.[19]

The overall aim of this study was to provide general guidelines on the effective design and synthesis of HexNAcase inhibitors and to show their applicability to human disease treatment. Variations in ring size, stereochemistry, presence of substituents along with cross-comparison relative to previously synthesized inhibitors allowed us to identify the essential interactions of the inhibitors with the HexNAcase active site. In particular ring contraction allowed us to identify the key functional groups essential for inhibitory activity. The reduction in ring size also had the side effect of making the inhibitor more atom- and synthetically step-efficient and reduced the complexity of the inhibitors due to the lower number of stereocenters involved.

Molecular modelling was used to rationalize the observed activity of the lower ring homologues. Furthermore predictions for future inhibitors were made based on the established model. Using these results in combination with further molecular modelling we were able to predict that of pipecolic amide **10** the substituents of C2, C3 and C6 need to be preserved without change, while C4 and C5 could be used for derivatization. Such analogues could be used to tune further properties of the inhibitors like biodistribution, oral availability and cellular uptake. In order to trial such a derivatization the ring nitrogen of pyrrolidine **11** was modified with a variety of substituents, due to the relative ease of synthetic access *via* reductive amination and the degree of cellular and organelle penetration was measured using a HPLC based free-oligosaccharide (FOS) assay. Finally with a supply of potent HexNAc inhibitors in hand, we investigated their biological activity in a cellular Boyden chamber experiment, to show their applicability to anti-cancer treatment.

Results and discussion

The following iminosugars were synthesised in addition to support our structure activity study of HexNAc inhibitors.

Synthesis of pipecolic amides 10 and 13

Two epimeric pipecolic amides **10** and **13**, both derived from D-mannose, were investigated. Azido lactone **15** (Scheme 1), previously employed in the synthesis of diastereomers of homonojirimycin,[20] was the common key intermediate. Selective protection to leave only the C6 hydroxyl group free followed by oxidation and reductive amination between C2 and C6 with retention of the stereochemistry at both centres would lead to the bicyclic intermediate **16**. Lactone opening with methylamine followed by global deprotection would then allow access to pipecolic amide **10**. The lead compound, pipecolic amide **10**, previously synthesised by Shilvock *et al.*,[17] has been shown to be a potent β-hexosaminidase inhibitor [K_i 0.01 μM, human placenta].

The C6-epimer **13** of pipecolic amide **10** could be synthesised in a similar fashion from the related bicycle **17**.[22] In this case inversion of configuration at C6 of the azidolactone **15** was now required. Selective deprotection of the terminal/primary acetonide of azidolactone **15** followed by selective silyl protection gave **18** (92% yield over 2 steps, Scheme 2) in which

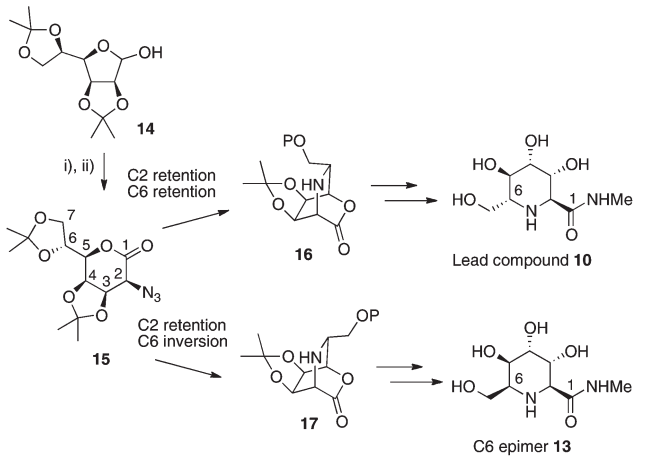

Scheme 1 General strategy towards pipecolic amides. (i) Lit.[21] NaCN, H_2O, $NaHCO_3$, then H_2SO_4; (ii) Tf_2O then NaN_3 introduced with retention.

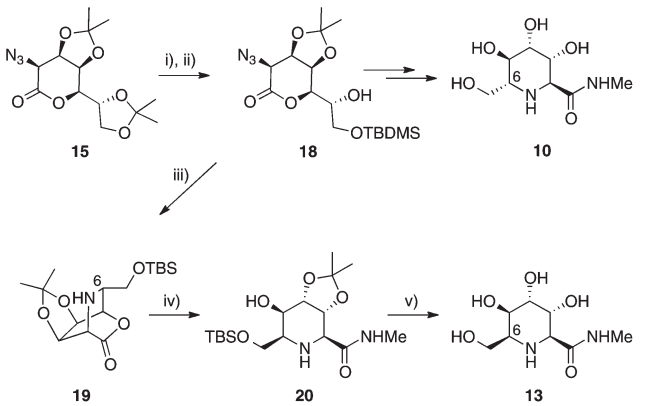

Scheme 2 Conditions: (i) aq. AcOH, 2.5 h, quant.; (ii) $Me_2tBuSiCl$, imidazole, DMF, RT, 18 h, 92%; (iii) Tf_2O, Pyr, DCM, −30 to −20 °C; then H_2, 10% Pd/C, NaOAc, EtOAc, 87%; (iv) $MeNH_2$, THF, RT, 75%; (v) MeOH/HCl, rt, 60%.

the C6-hydroxyl group is free. Subsequent activation of the C6 hydroxyl as the trifluoromethylsulfonate allowed inversion *via* an internal S_N2 displacement following reduction of the C2 azide functionality to give bicycle **19** in 87% yield (Scheme 2). Lactone opening with methylamine gave amide **20** (75%) and global deprotection under acidic conditions afforded the desired epimeric pipecolic amide **13** (60% yield).

Synthesis of pyrrolidine amide 21

The synthesis of all 16 5-hydroxymethyl-3,4-dihydroxyproline amides has previously been reported.[16] The most active β-hexosaminidase inhibitor of these was shown to be manno-amide **11** (Fig. 1) [K_i 0.027 μM HL60 cell homogenate]. In order to probe the importance of the presence of the CH_2OH side chain lyxonamide **21** (Scheme 3) was synthesised.

Lyxonamide **21** was accessed from the azido diol **22** which can readily be synthesised in 3 steps from D-lyxonolactone

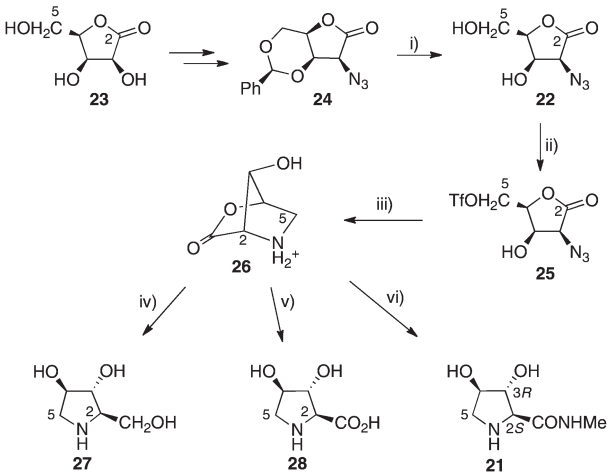

Scheme 3 (i) TFA, 1,4-dioxane, H_2O, RT, 88%; (ii) Tf_2O, Pyr, THF, −30 to −10 °C; (iii) H_2, Pd (black), EtOAc; (iv) $NaBH_4$, EtOH, 63% over 3 steps (v) 2 M HCl, 90% over 3 steps; (vi) $MeNH_2$, MeOH, 58% over 3 steps.

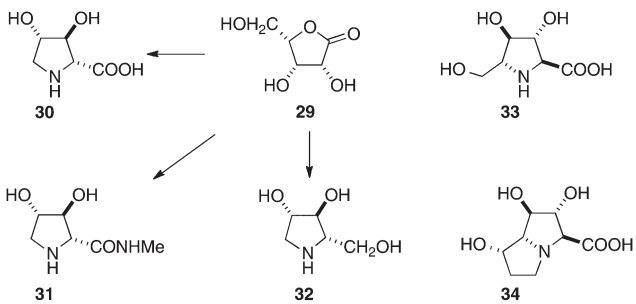

Scheme 4 Synthesis of the enantiomeric iminosugars.

23.[23] Selective activation of the primary hydroxyl of **22** as the trifluoromethanesulfonate followed by hydrogenolysis resulted in formation of bicyclic intermediate **26** (Scheme 3). Subsequent ring opening with methylamine in methanol gave the desired lyxonamide derivative **21** (58% over 3 steps from **22**). The bicyclic intermediate was additionally used to access the iminosugar DAB **27**, by reductive ring opening of the lactone (63% over 3 steps from **22**), and the corresponding amino acid **28**, by acid catalysed hydrolysis (90% over 3 steps from **22**).

In a similar manner L-lyxonolactone **29** was used as a starting material to provide access to the enantiomeric iminosugars **30**, **31** and **32** (Scheme 4).

Derivatives of D-manno-amide pyrrolidine 11

The most potent inhibitor was the amide **11**[16] of DMDP-related amino acid **33** (Scheme 4).[15] 7a-Epialexaflorine **34**, a conformationally restricted equivalent of **33**, has been isolated from leaves of *Alexa grandiflora*.[24] *N*-Alkylation has previously been seen to affect both the inhibitory profile of iminosugars and their cell penetration ability.[12b] Based on the previous study the *N*-butyl and *N*-hydroxyethyl derivatives were selected

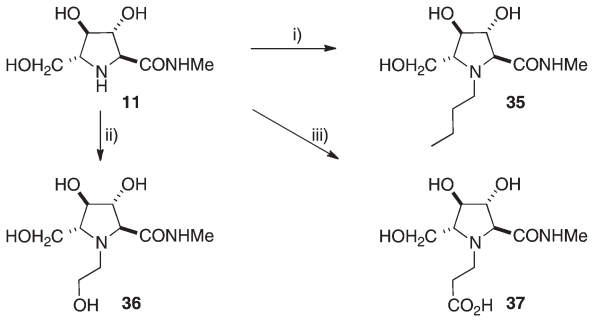

Scheme 5 (i) Butyraldehyde, 10% Pd/C, H_2, 1,4-dioxane, H_2O, 88%; (ii) glycolaldehyde dimer, 10% Pd/C, H_2, 1,4-dioxane, H_2O, 93%; (iii) *t*-Butylacrylate, MeOH, 55 °C; then TFA, H_2O, RT, 99%.

for investigation along with the *N*-propionic acid derivative. The *N*-butyl and *N*-hydroxyethyl compounds were synthesised *via* reductive aminations with butyraldehyde and glycolaldehyde dimer respectively to give **35** (88%) and **36** (93%) (Scheme 5); whereas the propionic acid derivative **37** was synthesised *via* a Michael addition with *t*-butylacrylate followed by acidic hydrolysis (99% over 2 steps).

Enzymatic evaluation and cross comparison of NH iminosugars

With the epimeric pipecolic amides **10** and **13**, the six pyrrolidines **11**, **21**, **31**, **38**, **39** and **40** and the azetidines **12** and **41** [18] in hand, we proceeded to perform a cross comparison of their inhibition profiles against β-*N*-acetylglucosaminidase, α-*N*-acetylgalactosaminidase and β-*N*-acetylgalactosaminidase, the results of which are listed in Tables 1 and 2. Based on this cross comparison the following conclusions can be drawn:

The methyl amide group may be a bioisostere of the CH_2NHAc group as can be seen when comparing the enzymatic inhibition of pyrrolidine **11** and ADMDP **6** and similarly when comparing azetidine amide **12** with azetidine NHAc **9** (Fig. 1). This has been shown in general when comparing pyrrolidine amides with their corresponding ADMDP-acetamide counterparts.[16,25]

With this bioisostere comparison established, the structural requirement for inhibition activity in form of the 2*S*,3*R* *trans*-motif between the hydroxyl and nitrogen containing functional group emerges. [This has been highlighted in red for known potent HexNAc inhibitors in Fig. 1 and similarly for structures contained in Tables 1 and 2.] The 6-ring **10** and 5-ring **11** are particularly active inhibitors displaying this 2*S*,3*R* *trans*-motif with a K_i of 0.01 μM (human placenta)[17] and 0.027 μM (HL60) respectively.

The completely inactive pipecolic amide **13** (Table 2) is exempt from this generalisation, pointing to the importance of the CH_2OH for potent inhibition. This encouraged us to probe deeper into the importance of the CH_2OH side chain in the 5-ring system. Epimerisation of CH_2OH at C5 in pyrrolidine **11** gave pyrrolidine **38** with a >20-fold (human placenta, 5.3 μM) reduction in inhibition. While complete removal of the CH_2OH group in pyrrolidine **21** was shown to be a 50-fold weaker inhibitor than **11** with an IC_{50} of 13 μM (human placenta).

Azetidine **12** containing a novel 4 membered ring scaffold, which has been shown to be stable for more than 6 months in aqueous solution, showed comparable inhibition to pyrrolidines **38** and **21** (Table 1).[18]

The enantiomeric iminosugars **31**, **39**, **40** and **41** shown in Table 2 all displayed considerably weaker inhibition profiles, consistent with the absence of the 2*S*,3*R* *trans*-motif.

Table 1 Concentration of iminosugars with 2*S*,3*R* configuration giving 50% inhibition of various glycosidases

	IC_{50} in μM [K_i in μM]				
	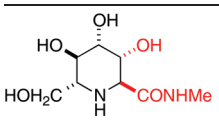	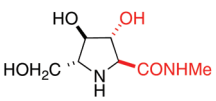	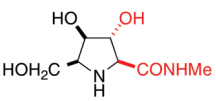	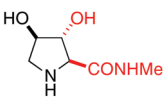	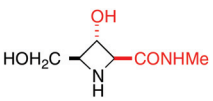
Enzyme	**10**	**11**	**38** [16]	**21**	**12**
β-*N*-Acetylglucosaminidase					
Aspergillus oryzae	49	0.30	6.6	47	64
Bovine kidney	0.27	0.22	4.8	9.7	2.7
HL60	0.36	0.20 [K_i = 0.027]	6.1 [K_i = 14.9]	16 [K_i = 42.5]	5.2 [K_i = 0.89]
Human placenta	0.14 [K_i = 0.01][c]	0.20	5.3	13	4.3
Jack bean	0.29	0.033	1.2	9.1	4.2
α-*N*-Acetylgalactosaminidase					
Charonia lampas	NI[b] (0%)	NI[b] (1.0%)	NI[b] (9.0%)	NI[b] (5.4%)	NI[b] (15.3%)
Chicken liver	NI[a] (0%)	NI[a] (0%)	NI[a] (0%)	NI[a] (5.1%)	NI[a] (0%)
β-*N*-Acetylgalactosaminidase					
Aspergillus oryzae	26	0.35	7.3	57	36
HL60	1.8	1.0	26	21	20

[a] NI: no inhibition (less than 50% inhibition at 1000 μM); (): inhibition % at 1000 μM. [b] NI: no inhibition (less than 50% inhibition at 500 μM); (): inhibition % at 500 μM. [c] []: data from Shilvock *et al.*, 1998.[17]

Table 2 Concentration of enantiomeric (**31**, **39**, **40**, **41**) and epimeric (**13**) iminosugars giving 50% inhibition of various glycosidases

	IC_{50} in μM				
	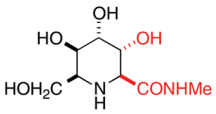	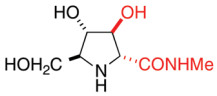	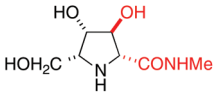	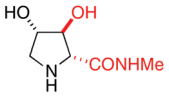	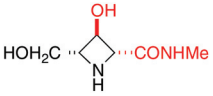
Enzyme	**13**	**39** [16]	**40** [16]	**31**	**41** [18]
β-*N*-Acetylglucosaminidase					
Aspergillus oryzae	NI[a] (0.0%)	53	NI[a] (9.3%)	NI[a] (0.4%)	NI[a] (21.4%)
Bovine kidney	NI[a] (28.9%)	32	566	NI[a] (5.2%)	NI[a] (46.8%)
HL60	NI[a] (14.5%)	50 [K_i = 75.1]	849	NI[a] (8.4%)	NI[a] (34.7%)
Human placenta	NI[a] (24.7%)	41	584	NI[a] (3.3%)	NI[a] (42.8%)
Jack bean	NI[a] (21.3%)	7.3	119	NI[a] (8.3%)	797
α-*N*-Acetylgalactosaminidase					
Charonia lampas	NI[b] (14.4%)	NI[b] (1.8%)	NI[b] (4.7%)	NI[b] (3.5%)	NI[a] (13.9%)
Chicken liver	NI[a] (0%)	NI[a] (9.6%)	NI[a] (10.0%)	NI[a] (3.1%)	NI[a] (12.5%)
β-*N*-Acetylgalactosaminidase					
Aspergillus oryzae	NI[a] (8.7%)	84	NI[a] (9.6%)	NI[a] (0.4%)	NI[a] (26.0%)
HL60	NI[a] (10.6%)	206	NI[a] (30.2%)	NI[a] (1.8%)	NI[a] (11.3%)

[a] NI: no inhibition (less than 50% inhibition at 1000 μM); (): inhibition % at 1000 μM. [b] NI: no inhibition (less than 50% inhibition at 500 μM); (): inhibition % at 500 μM.

Crystal structures of HexB derived from human placenta with either of the known inhibitors GalNAc-isofagamine or NAG-thiazoline (Fig. 2) have been obtained[19a] and demonstrate that the active site of this hexosaminidase can accommodate inhibitors with both *gluco* and *galacto* configurations. It can be seen that the inhibitors share several of the key structural features namely a similar *trans*-relationship between the nitrogen containing functional group and both the neighbouring hydroxyl and the exocyclic hydroxymethyl group.

Based on the enzymatic evaluation the following essential SARs for HexNAc inhibitors emerge:

1. The methyl amide group may be a good bioisostere of CH_2NHAc.
2. A *trans*-relationship between C3-OH and C2-CONHMe in a 2*S*,3*R* motif.
3. The presence of an exocyclic CH_2OH group in a *trans*-relationship relative to C2–CONHMe.

The modelling section of this manuscript aims to further rationalize these observations.

The iminosugars were found to have a high selectivity against hexoaminidases, screening against the standard panel of glycosidases showed no significant activity (for full tables of data see ESI†).

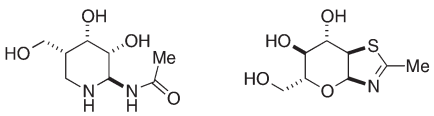

Fig. 2 Structures of known inhibitors of HexB with *galacto* and *gluco* configurations.[19a]

Enzymatic evaluation of *N*-alkylated derivatives of pyrrolidine 11

The most potent 5-ring iminosugar **11** was modified *via* alkylation on the ring nitrogen to give the butyl- **35**, hydroxyethyl- **36** and carboxyethyl- **37** derivatives and subjected to the same enzyme panel (Table 3). *N*-Alkylation of **11** led to a decrease in inhibitory activity against β-*N*-acetylglucosaminidase. All the derivatives **35**, **36** and **37** gave very comparable levels of inhibition with K_is of 1.31 μM, 0.72 μM and 1.08 μM respectively (HL60).

Free oligosaccharide analysis to establish cellular uptake

The *N*-alkylated pyrollidine amides **35**, **36** and **37** along with the parent compound **11** were subjected to free oligosaccharide analysis to evaluate differences in cellular uptake.[26] The general concept for this assay is outlined in section 4 of the ESI.† The side chain derivatives of the 5-ring show the same general trends that were previously observed in the 6-ring system DGJNAc **5**.[12b] The hydrophobic *N*-butyl side chain promoted cellular uptake of the iminosugar, whereas the hydrophilic hydroxyethyl or carboxylic acid modifications restricted the inhibitors to extracellular space. It was found that at 50 μM the *N*-butyl derivative **35** was 5-fold more efficient at inhibiting β-*N*-acetylglucosaminidase on a cellular level than the propionic derivative **37** (Fig. 3C) and 10-fold more effective then the hydroxyethyl derivative **36** on a cellular level, despite having very comparable levels of inhibition on a enzymatic level. Even at 200 μM concentrations (Fig. 3D) this difference in cellular penetration can still be detected. This establishes the influence of iminosugar ring nitrogen derivatisation as a point of manipulating cell penetration as a more universal concept.

A detailed table of results from the FOS analysis of the individual labelled glycans in terms of glucose units can be found in the ESI.†

Table 3 Concentration of pyrrolidine amide **11** and derivatives giving 50% inhibition of various glycosidases

	IC_{50} in μM			
	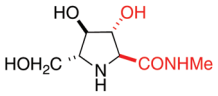	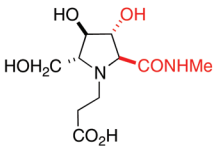	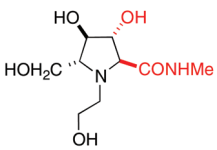	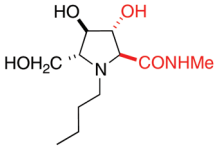
Enzyme	**11**	**37**	**36**	**35**
β-*N*-Acetylglucosaminidase				
Human placenta	0.20	1.9	4.8	1.1
Bovine kidney	0.22	2.7	6.3	1.5
Jack bean	0.033	0.41	1.8	0.35
HL 60	**0.2 [K_i = 0.027]**	**1.6 [K_i = 1.08]**	**4.9 [K_i = 0.72]**	**1.4 [K_i = 1.31]**
Aspergillus oryzae	0.30	3.4	17	0.83
α-*N*-Acetylgalactosaminidase				
Charonia lampas	NI[a] (1.0%)[c]	NI[a] (15.9%)[c]	NI[a] (1.6%)[c]	NI[a] (0%)[c]
Chicken liver	NI[a] (0%)[b]	NI[a] (9.8%)[b]	NI[a] (20.8%)[b]	NI[a] (7.9%)[b]
β-*N*-Acetylgalactosaminidase				
HL60	1.0	7.9	15	3.9
Aspergillus oryzae	0.35	3.7	16	0.79

[a] NI: no inhibition (less than 50% inhibition at 1000 μM). [b] (): inhibition % at 1000 μM. [c] (): inhibition % at 500 μM.

Molecular modelling

With the enzymatic inhibition of HexNAcase established, it was of interest to see if the observed activity of inhibitors **10**, **11**, **12** and **21** could be rationalized using molecular modelling and if predictions for future inhibitors based on the model were possible.

Density functional theory (DFT) methods were used to calculate the lowest energy conformations of the iminosugar inhibitors. These structures were then overlayed to enable shape based analogies to be drawn. Calculations in this study were performed at the M06-2X[27] level of theory, which has shown impressive results for main group chemistry and is an improvement on the popular B3LYP method.[28]

In a previous study on a highly strained azetidine system we established that structures calculated with this method agreed very well with the corresponding structure determined by X-ray crystallography.[29] To determine shape based similarities, the structures to be compared were overlayed by their heteroatoms (hydroxyl-, amide and ring nitrogen functionality), which are presumed to be the important points of interaction with the active site of the HexNAcase enzyme.

With the importance of the C2, C3 *trans* motif firmly established, the hypothesis that the C6 hydroxymethyl group of amide **10** was necessary for good inhibitory activity and the significance of the C4 and C5 stereocenters was further investigated.

Importance of stereocenters – eliminating C4

To establish the structural similarity between inhibitors with high levels of activity (Table 1) we compared pipecolic amide **10** and pyrrolidine **11**. Fig. 4 shows that the two structures overlay favourably. The 5-ring system essentially represents a cut down version of the 6-ring analogue by excision of the C4 carbon. We can therefore conclude that C4 is less crucial for providing potent inhibition.

Importance of stereocenters – eliminating C4 and C6

Azetidine **12** is a further ring contraction of the highly active pyrrolidine **11**, but despite retaining a CH_2OH functionality, the overlay in Fig. 5 clearly shows that relative to pyrrolidine **11** the azetidine **12** preserves the interaction points of C4–OH, C3–OH and amide functionality rather than the C6–OH from the CH_2OH group. Relative to the 6-ring pipecolic amide **10**, the azetidine therefore eliminates C4 and C6 from the structure preserving the interactions of C5–OH, C3–OH and C2–CONHMe respectively.

Azetidine **12** can also be understood as a ring contraction (Fig. 6) of the pyrrolidines **21** or **38** with the hydroxymethyl of **12** correlating to the C4–OH of the other two structures. This would explain the comparable levels of enzymatic inhibition displayed by **38**, **21** and **12**.

In conclusion the molecular modelling study and SAR data rationalize the importance of the correct orientation and presence of the exocyclic CH_2OH group, *trans* to the C2 amide; as well as the *trans*-C2, C3 relationship, in both pipecolic and pyrrolidine amides. The C4, and to a reduced extent C5, hydroxyl groups emerge as being less crucial for activity and could potentially therefore tolerate modification.

Based on this model we predict *trans*-azetidine **42** to be a potentially potent inhibitor as it would preserve both the *trans*-2*S*,3*R* motif of C2 and C3 and maintain the presence of the CH_2OH sidechain *trans* across the ring to the amide group (Fig. 7), both of which have been shown here to be key requirements for potent HexNAc activity in this study. Although

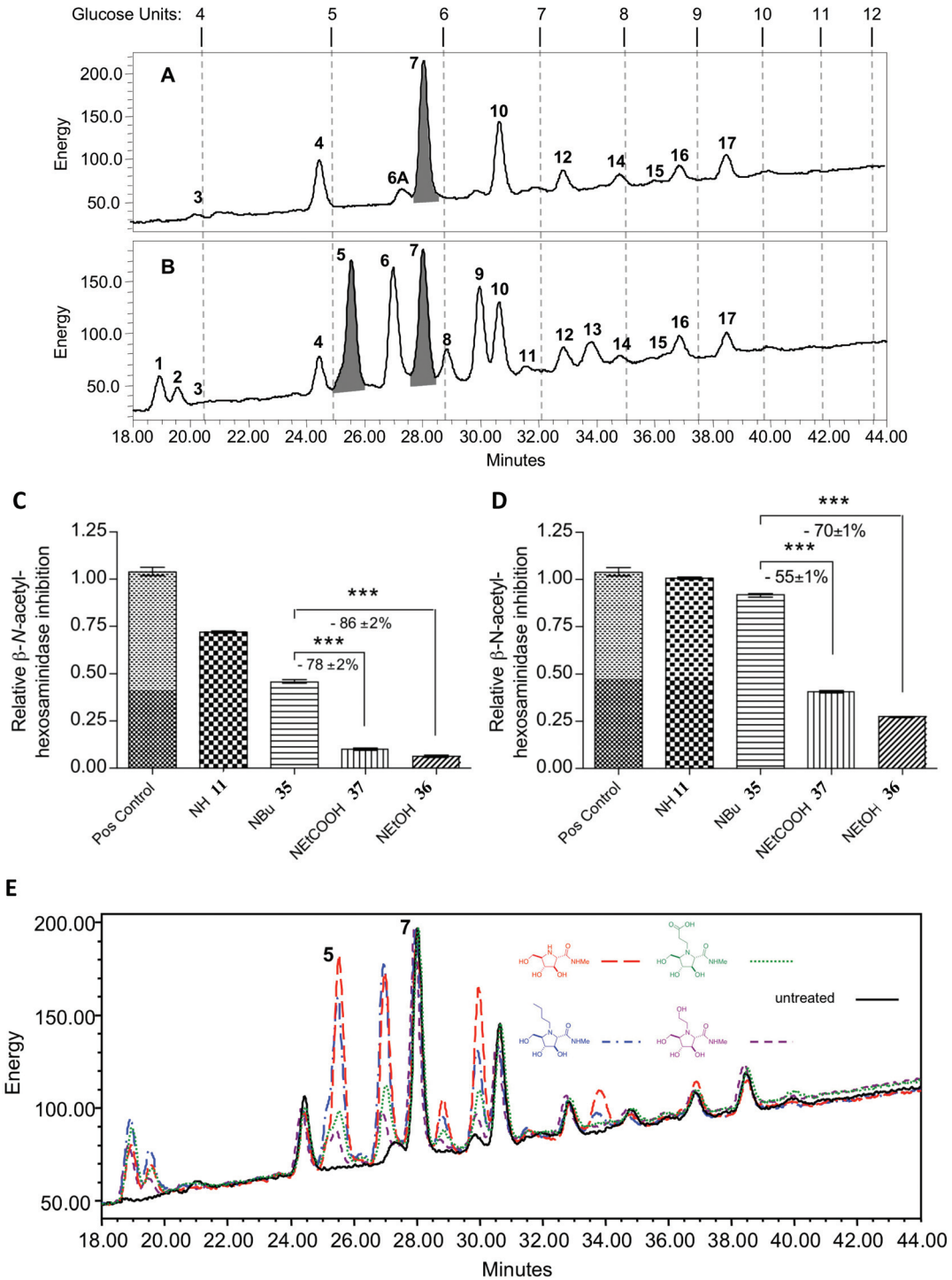

Fig. 3 HL60 cells were homogenized and the free oligosaccharides (FOS) extracted as described in the experimental section. After 2-AA labelling the FOS were separated using HPLC. (A) shows the profile of untreated cells while (B) shows cells treated with 200 μM of DGJNAc **5**. Peaks have been numbered and their structure given in the ESI.† The ratio of the areas of peak 5 and peak 7 were used to gage β-hexosamindase inhibition on a cellular level. A high ratio indicates high levels of inhibition. (C) Inhibitor concentrations at 50 μM. Positive control DGJNAc **5** at 200 μM. (D) Inhibitor concentrations at 200 μM. Positive control DGJNAc **5** at 200 μM. Decreases in inhibition relative to butyl derivative **35** indicated in % with S.D. (E) Overlay of HPLC traces with all inhibitors at 200 μM in comparison to untreated cells indicating the variation in peak 5 in comparison to control peak 7.

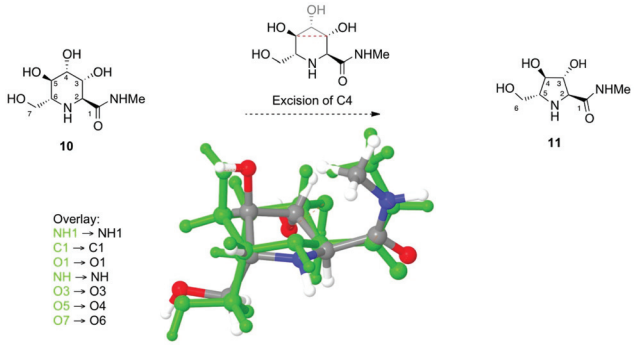

Fig. 4 Shape based comparison between highly active HEXNAc inhibitors – overlay of 6-ring **10** with 5-ring **11**. 6-ring shown in green, 5-ring in colour: grey – C, red – O, blue – N and white – H. Amide functionality overlayed and overlapping oxygens indicated with dashed red lines.

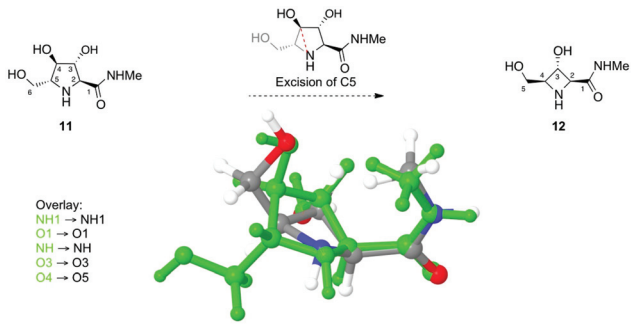

Fig. 5 Shape based comparison between manno 5-ring **11** (green) and *cis*-azetidine **12** (colour).

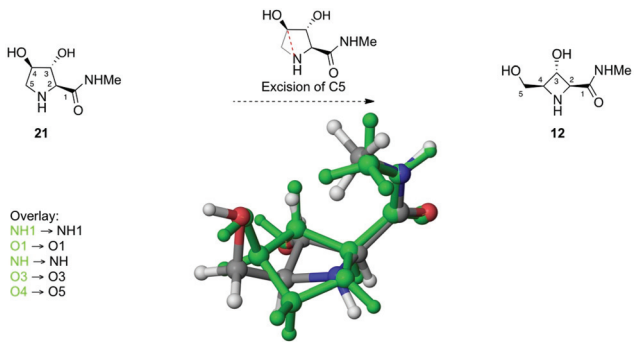

Fig. 6 Shape based comparison between 5-ring **21** (green) and *cis*-azetidine **12** (colour).

azetidines where the two side chains are in a *cis*-relationship are readily available,[16,18,30] all attempts at the synthesis of azetidines with a *trans*-relationship of those two groups have been unsuccessful.[31]

HexNAc inhibitors and anti-cancer applications

With several potent HexNAc inhibitors in hand we wanted to establish if their anti-invasive properties could be established in an *in vitro* assay.

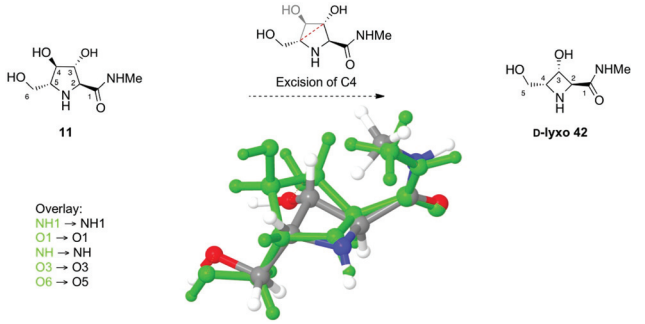

Fig. 7 Activity prediction of *trans*-azetidine **42** due retention of both C2, C3 *trans* relationship and CH_2OH sidechain. Overlay of manno 5-ring **11** (green) and *trans*-azetidine **42** (colour).

The process of metastasis formation is a complex process of sequential steps (see section 5 in ESI† for overview). As the overall process involves the degredation of the ECM on two occasions protection of the ECM could be a viable anti-cancer strategy halting the progression of the disease. Cancer cells secret a cocktail of enzymes to digest the ECM including β-*N*-acetyl-hexosaminidases.[32] Previous studies on HexNAc inhibitors have shown that these inhibitors have the potential to protect the ECM.[6,7b,33] Therefore the potential of the HexNAc inhibitor D-manno-amide **11** to be a cytostatic anti-metastasis agent was investigated.

The QCM™ 24-well cell invasion assay (Millipore) was used as a Boyden chamber type assay (for description see section 5 in ESI†) which employs a fluorescence based detection method for quantifying the number of invaded cells.[34] The most invasive breast cancer cell line previously found in a Boyden chamber set-up, MDA-MB-231, was used.[35]

As a mixture of enzymes is secreted an approach using the combination of inhibitors for a range of different biological targets might be the most useful. In this case the highly active pyrrolidine HexNAc inhibitor **11** was studied along with the established proteinase inhibitor Marimastat **43**[36] – both independently and in combination (Fig. 8). A 3 μM concentration of Marimastat **43** was required to obtain a 70% reduction of invasion, with a 24 h incubation period, when used as a single agent in this study. The iminosugar **11** at a 500 μM concentration was seen to have only a minor contribution under these conditions, however, on increasing the incubation time to 64 h, although reducing the overall anti-invasive effects of the inhibitors, the contribution of the iminosugar appeared more pronounced. The iminosugar and marimastat, as single agents, decreased the invasiveness of the breast cancer cells by 16% and 25% respectively, while in combination a far greater reduction was shown, indicating that the effect of the inhibitors is additive.

Interestingly the effect of the iminosugar was maintained at concentrations down to 5 μM. At an incubation time of 48 h a 5 μM dose of iminosugar **11**, as a single agent, reduced the invasiveness of MDA-MB-231 cells by 29%.

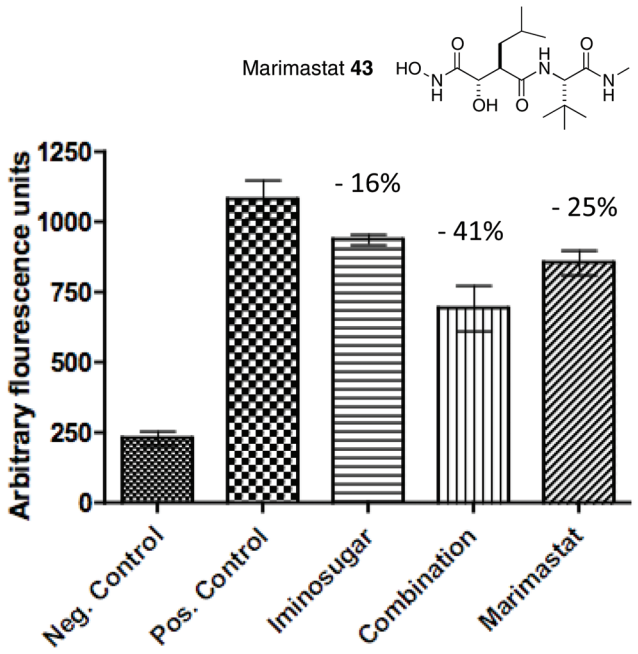

Fig. 8 Combination treatment of iminosugar **11** and MMP inhibitor **43** in cell invasion assay using MDA-MB-231 cells show additive effects; 820 000 cells per well; 24 h starvation; iminosugar **11** used at concentration of 500 μM; MMP inhibitor Mariamastat **43** at 3 μM; chemo-attractant is 10% FCS; negative control with no FCS; 64 h invasion time.

It was established that the D-manno-amide **11** was non-toxic to the cell line used (MTS assay data up to 1 mM concentration available in ESI†) and control experiments ruled out any assay interference of the fluorescent detection method by the iminosugar.

Conclusion

In summary, the structural features of the potent HexNAcase inhibitor, pipecolic amide **10** were investigated to determine which were essential for its inhibitory activity. The activity of pipecolic amide **10** and its epimer **13** were compared with that of the corresponding 5- and 4-membered iminosugar amides. The methylamide may be a good bioisostere of the NAc group. A *trans*-(2*S*,3*R*)-relationship between the C3–OH and C2-NAc or methylamide was required to be preserved throughout for HexNAcase inhibitory activity. Additionally the presence of an exocyclic CH_2OH sidechain increased the activity especially if in a *trans*-relationship relative to the C2–CONHMe. The C4, and to a lesser extent C5, hydroxyl groups emerged as being less crucial for activity and therefore could be used as sites for modification. Molecular modelling was used to rationalize the observed activity of the lower ring homologues and predicted that the C2/C4-*cis* azetidine amide **42** should be a potent HexNAcase inhibitor.

The degree of cellular and organelle penetration was measured on a variety of *N*-substituted derivatives of manno-amide **11** indicating that hydrophilic side chains restrict cellular access, while hydrophobic side chains favour cellular uptake. In addition, initial studies showed that the manno-amide **11**, in combinatorial treatment with a protease inhibitor, was able to reduce invasiveness of the highly aggressive breast cancer cell line MDA-MB-231.

Experimental section

All commercial reagents were used as supplied. Thin layer chromatography (TLC) was performed on aluminium sheets coated with 60 F_{254} silica. Plates were visualized using a spray of 0.2% w/v cerium(IV) sulfate and 5% ammonium molybdate solution in 2 M aqueous sulfuric acid. Flash chromatography was performed on Sorbsil C60 40/60 silica. Melting points were recorded on a Kofler hot block and are uncorrected. Optical rotation concentrations are quoted in g per 100 mL. ^{1}H and ^{13}C NMR spectra were assigned by utilizing 2D COSY and HSQC spectra. All chemical shifts (δ) are quoted in ppm and coupling constants (J) in Hz. Residual signals from the solvents were used as an internal reference.[37] For solutions in D_2O acetonitrile was used as an internal reference. HRMS measurements were made using a microTOF mass analyzer.

Chemical experimental section

C6 epimer of Shilvock pipecolic amide 13

7-O-tert-Butyldimethylsilyl-2,6-dideoxy-2,6-imino-3,4-O-isopropylidene-L-glycero-D-talo-heptono-1,5-lactone ***19***. To a stirred solution of alcohol **18** (321 mg, 0.83 mmol) in dichloromethane (10 mL) at −30 °C was added pyridine (0.18 mL, 1.08 mmol) and trifluoromethanesulfonic anhydride (0.2 mL, 2.48 mmol). The reaction mixture was allowed to warm to −20 °C; after 1.5 h t.l.c. analysis (4 : 1, cyclohexane/ethyl acetate) indicated conversion of the starting material (R_f 0.14) to one major product (R_f 0.46). The reaction mixture was diluted with dichloromethane (13 mL) and washed with dilute aq. hydrochloric acid (2 × 5 mL), brine (60 mL) and dried ($MgSO_4$). The organic layer was evaporated to dryness and the crude reaction product was used without further purification in the next reaction step. The crude triflate (0.43 g, 0.83 mmol) in ethyl acetate (15 mL) was stirred vigorously at rt under hydrogen in the presence of anhydrous sodium acetate (0.27 g, 3.31 mmol) and 10% palladium on charcoal (10% by weight, 45 mg). After 16 h the mixture was filtered through celite, washed with ethyl acetate (15 mL) and evaporated to dryness. The crude product **19** was purified *via* flash column chromatography (1 : 1, cyclohexane/ethyl acetate) and the product was isolated as a clear oil (246 mg, 0.72 mmol, 87%); HRMS (ESI +ve): found 366.1704 ($[M + Na]^+$); $C_{16}H_{29}NNaO_5Si$ requires 366.1707; $[\alpha]_D^{25}$ −7.0 (c 1.30, $CHCl_3$); ν_{max} (thin film): 3514 (br, N–H), 1770 (s, C=O); δ_H (400 MHz, $CDCl_3$): 0.05 (6H, s, $Si(CH_3)_2$), 0.88 (9H, s, $SiC(CH_3)_3$), 1.40 (3H, s, CH_3), 1.60 (3H, s, CH_3), 3.53–3.45 (3H, m, H6, H7, H7′), 3.67 (1H, d, H2, $J_{2,3}$ 3.0), 4.38 (1H, dd, H3, $J_{3,2}$ 3.0, $J_{3,4}$ 8.0), 4.51 (1H, dd, H4, $J_{4,5}$ 4.3, $J_{4,3}$ 8.0), 4.83 (1 H, d, H5, $J_{4,5}$ 4.3); δ_C (100.6 MHz, $CDCl_3$): −5.4 ($SiCH_3$), −5.3 ($SiCH_3$), 18.4 $SiC(CH_3)_3$, 24.6 ($C(CH_3)_2$),

26.0 ($SiC(\underline{C}H_3)_3$), 26.1 ($C(\underline{C}H_3)_2$), 48.6 (C6), 54.3 (C2), 62.8 (C7), 71.5 (C4), 72.7 (C3), 74.9 (C5), 113.9 ($\underline{C}(CH_3)_2$), 170.6 (C1); *m*/*z* (ESI +ve): 709 ($[2M + Na]^+$, 100%).

Methyl 7-O-tert-butyldimethylsilyl-2,6-dideoxy-2,6-imino-3,4-O-isopropylidene-L-glycero-D-talo-heptonamide ***20***. To a solution of bicycle **19** (111 mg, 0.32 mmol) in dry tetrahydrofuran (2 mL) under nitrogen, methylamine (33 w/w% solution in industrial methylated spirit, 0.12 mL) was added. After 18 h t.l.c. analysis (ethyl acetate, starting material R_f 0.90, product R_f 0.32) indicated that the reaction had gone to completion and the mixture was concentrated to dryness. The residue was purified *via* flash column chromatography (5 : 1, ethyl acetate/cyclohexane) and amide **20** was isolated as colourless oil (91 mg, 0.242 mmol, 52%); HRMS (ESI +ve): found 397.2115 ($[M + Na]^+$); $C_{17}H_{34}N_2NaO_5Si$ requires: 397.2129; $[\alpha]_D^{25}$ +48.5 (*c* 0.63, $CHCl_3$); ν_{max} (thin film): 3344 (br, OH, NH), 1657 (s, amide I), 1545 (m, amide II); δ_H (400 MHz, $CDCl_3$): 0.08 (6H, d, $Si(CH_3)_2$, *J* 1.8), 0.90 (9H, s, $SiC(CH_3)_3$), 1.39 (3H, s, $C(CH_3)_2$), 1.54 (3H, s, $C(CH_3)_2$), 2.84 (3H, d, NH<u>Me</u>, $J_{Me,NH}$ 4.8), 3.03 (1H, a-t, H6, *J* 5.1), 3.13 (1H, d, OH, $J_{OH,5}$ 6.2), 3.28 (1H, d, H2, $J_{2,3}$ 8.4), 3.79 (1H, dd, H7, $J_{7,6}$ 6.6, $J_{7,7'}$ 10.0), 3.83 (1H, dd, H7′, $J_{7',6}$ 4.3, $J_{7',7}$ 10.0), 3.94 (1H, a-s, H5), 4.22 (1H, dd, H3, $J_{3,4}$ 5.1, $J_{2,3}$ 8.4), 4.25 (1H, dd, H4, $J_{4,5}$ 2.4, $J_{4,3}$ 5.1), 6.50 (1H, br. a-d, NH, $J_{NH,Me}$ 3.6); δ_C (100.6 MHz, $CDCl_3$): −5.3 ($Si(CH_3)_2$), 18.4 ($Si\underline{C}(CH_3)_3$), 26.0 ($SiC(\underline{C}H_3)_3$), 26.2 ($C(\underline{C}H_3)_2$, NHMe), 28.4 ($C(\underline{C}H_3)_2$), 56.7 (C6), 61.0 (C2), 64.5 (C7), 67.3 (C5), 73.4 (C3), 77.3 (C4), 110.1 ($\underline{C}(CH_3)_2$), 172.2 (C1); *m*/*z* (ESI +ve): 771 ($[2M + Na]^+$, 100%).

Methyl 2,6-dideoxy-2,6-imino-L-glycero-D-talo-heptonamide ***13***. Amide **20** (53 mg, 0.14 mmol) was stirred in 3% methanolic hydrochloric acid (generated from acetyl chloride 0.3 mL with 9.7 mL methanol at 0 °C) at rt for 18 h. The solution was concentrated *in vacuo* and coevaporated with methanol (3 × 10 mL). The residue was purified by ion exchange chromatography (Amberlite IR-120, H^+ form, eluting with 1.0 M aq. ammonium hydroxide). T.l.c. analysis showed a single spot (DONALD, 14 : 3 : 1 : 1 : 1, ethanol/pyridine/*n*-butylalcohol/acetic acid/water R_f 0.52). Amide **13** was isolated as a colourless oil (18 mg, 0.084 mmol, 60%); HRMS (ESI +ve): found 243.0951 ($[M + Na]^+$); $C_8H_{16}N_2NaO_5$ requires: 243.0951; $[\alpha]_D^{25}$ +27.3 (*c* 0.75, H_2O); ν_{max} (thin film): 3316 (br, O–H), 1650 (s, amide I), 1562 (m, amide II); δ_H (400 MHz, D_2O): 2.67 (3H, s, NHMe) 2.98 (1H, a-t, H6, *J* 6.5), 3.23 (1H, s, NH), 3.32 (1H, d, H2, $J_{2,3}$ 10.4), 3.51 (1H, dd, H7, $J_{7,6}$ 4.9, $J_{7,7'}$ 9.4), 3.55 (1H, dd, H7′, $J_{7',6}$ 5.0, $J_{7',7}$ 9.4), 3.87–3.77 (2H, m, H3, H5), 3.92 (1H, a-t, H4, *J* 3.4); δ_C (100.6 MHz, D_2O): 26.2 (Me) 53.7 (C6), 59.0 (C2), 61.2 (C7), 67.4 (C3), 69.2 (C5), 70.9 (C4), 173.5 (C1); *m*/*z* (ESI +ve): 243 ($[M + Na]^+$, 100%).

LAB and DAB amides 21 and 31

2-Azido-2-deoxy-D-lyxono-1,4-lactone ***22***. Benzylidene protected lactone **24** (1.71 g, 7.2 mmol) was dissolved in a mixture of trifluoroacetic acid (50 mL), 1,4-dioxane (50 mL) and water (50 mL) and stirred at rt for 4 h. After this time t.l.c. analysis (ethyl acetate) showed complete conversion of the starting material (R_f 0.60), to one major product (R_f 0.30). The reaction mixture was diluted with water (50 mL) and the solvent removed under reduced pressure, co-evaporating with water (5 × 25 mL) Purification by flash column chromatography (1 : 1, cyclohexane/ethyl acetate) yielded the unprotected lactone **22** (1.0 g, 88%) as a colourless oil; $[\alpha]_D^{25}$ +41.3 (*c* 0.60, H_2O) [Lit.[38] $[\alpha]_D^{20}$ +38.0 (*c* 0.25, H_2O)]; ν_{max} (thin film): 3385 (br. s, OH), 2120 (s, N_3), 1778 (s, C=O); δ_H (400 MHz, $(CD_3)_2CO$): 3.92 (2H, a-t, H5, H5′, *J* 5.6), 4.23 (1H, t, OH5, $J_{OH,5}$ 5.8), 4.39 (1H, d, H2, $J_{2,3}$ 4.6), 4.56 (1H, dt, H4, $J_{4,3}$ 2.8, $J_{4,5} = J_{4,5'}$ 5.8), 4.75 (1H, dt, H3, $J_{3,4}$ 2.8, $J_{3,2} = J_{3,OH}$ 4.6), 5.36 (1H, d, OH3, $J_{OH,3}$ 4.6); δ_C (100.6 MHz, $(CD_3)_2CO$): 59.7 (C5), 62.0 (C2), 70.9 (C3), 81.9 (C4), 171.5 (C1); *m*/*z* (ESI +ve): 174 ($[M + H]^+$, 100%).

[Enantiomer: *2-azido-2-deoxy-L-lyxono-1,4-lactone* $[\alpha]_D^{25}$ −21.9 (*c* 1.20, H_2O)].

2-Azido-2-deoxy-5-O-trifluoromethanesulfonyl-D-lyxono-1,4-lactone ***25***. Trifluoromethanesulfonic anhydride (0.34 mL, 2.0 mmol) was added dropwise to a stirred solution of azido-lactone **22** (0.33 g, 1.9 mmol) and pyridine (0.39 mL, 4.8 mmol) in dry tetrahydrofuran (10 mL) at −30 °C. The reaction was stirred for 1.5 h at −30 to −10 °C after which t.l.c. analysis (ethyl acetate) showed the presence of the starting material (R_f 0.30) and one major product (R_f 0.70). After a further 70 min t.l.c. analysis indicated only trace starting material remaining. The reaction mixture was partitioned between ethyl acetate (100 mL) and 2 M hydrochloric acid (100 mL). The organic layer was washed with water (100 mL) and brine (100 mL), dried ($MgSO_4$), filtered and the solvent removed under reduced pressure. Purification by flash column chromatography (1 : 1, cyclohexane/ethyl acetate) yielded the azido triflate **25** (0.38 g, 65%) as a white solid; m.p. 102 °C (decomp.); $[\alpha]_D^{25}$ +20.1 (*c* 1.38, acetone); ν_{max} (thin film): 2122 (s, N_3), 1790 (s, C=O); δ_H (400 MHz, $(CD_3)_2CO$): 4.57 (1H, d, H2, $J_{2,3}$ 4.6), 4.93 (1H, dd, H5, $J_{5,4}$ 8.1, $J_{5,5'}$ 11.0), 4.97 (1H, dd, H3, $J_{3,4}$ 3.0, $J_{3,2}$ 4.8), 5.05 (1H, dt, H4, $J_{4,5'} = J_{4,3}$ 2.8, $J_{4,5}$ 8.4), 5.16 (1H, dd, H5′, $J_{5',4}$ 2.5, $J_{5',5}$ 11.1), 5.78 (1H, br. s, OH); δ_C (100.6 MHz, $(CD_3)_2CO$): 62.4 (C2), 71.3 (C3), 76.5 (C5), 79.0 (C4), 121.1 (CF_3), 171.5 (C1); *m*/*z* (ESI +ve): 328 ($[M + Na]^+$, 100%).

[Enantiomer: 2-azido-2-deoxy-5-*O*-trifluoromethanesulfonyl-L-lyxono-1,4-lactone $[\alpha]_D^{25}$ −16.6 (*c* 1.07, acetone)].

2,5-Dideoxy-2,5-iminium-D-lyxono-1,4-lactone trifluoromethanesulfonate ***26***. Azido triflate **25** (0.29 g, 0.93 mmol) and palladium black (20 mg) were stirred in ethyl acetate (5 mL) at rt. The reaction vessel was purged under vacuum and charged with an atmosphere of hydrogen. The reaction was stirred for 2.5 h after which t.l.c. analysis (ethyl acetate) showed complete conversion of the starting material (R_f 0.70) to one major product (R_f 0.10). The catalyst was removed by filtration (glass microfibre) and the solvent removed under reduced pressure to give the triflate salt, **26** (0.14 g, quant.), as a red amorphous solid. The crude bicylic salt was used without further purification. Partial data for crude bicycle **26**: ν_{max} (thin film): 3455 (br. s, NH), 1814 (s, C=O); *m*/*z* (ESI +ve): 162 ($[M + MeOH]^+$, 90%).

Methyl 2,5-dideoxy-2,5-imino-D-lyxonamide ***21***. Methylamine (33 wt% in EtOH, 1.54 mL, 27.0 mmol) was added to a solution of the crude bicyclic triflate salt **26** (0.75 g, 2.7 mmol) in

methanol (10 mL). The reaction was stirred at rt for 1 h after which mass spectrometry indicated the presence of the product (*m*/*z* 161 $[M + H]^+$). The solvent was removed under reduced pressure and the residue loaded onto a short column of Dowex® (50 W X8, H^+). The column was washed with water and the product liberated with 2 M aqueous ammonia. The ammoniacal fractions were concentrated under reduced pressure to give the amide **21** (87 mg, 58% over 3 steps) as a brown oil; HRMS (ESI +ve): found 183.0741 ($[M + Na]^+$); $C_6H_{12}N_2NaO_3$ requires 183.0740; $[\alpha]_D^{25}$ −11.3 (*c* 0.20, H_2O); ν_{max} (thin film): 3356 (br. s, OH/NH), 1674 (s, C═O); δ_H (400 MHz, D_2O, HCl Salt): 2.81 (3H, s, NCH_3), 3.48 (1H, dd, H5, $J_{5,4}$ 1.8, $J_{5,5'}$ 12.6), 3.65 (1H, dd, H5′, $J_{5',4}$ 4.3, $J_{5',5}$ 12.6), 4.30 (1H, d, H2, $J_{2,3}$ 2.3), 4.35 (1H, dt, H4, $J_{4,3} = J_{4,5}$ 2.1, $J_{4,5'}$ 4.4), 4.45 (1H, t, H3, $J_{3,2} = J_{3,4}$ 2.2); δ_C (100.6 MHz, D_2O, HCl Salt): 26.8 (NCH_3), 51.5 (C5), 66.2 (C2), 76.7 (C4), 79.2 (C3), 166.1 (C1); *m*/*z* (ESI +ve): 183 ($[M + Na]^+$, 95%), 161 ($[M + H]^+$, 100%).

[Enantiomer: *methyl 2,5-dideoxy-2,5-imino-L-lyxonamide* **31** $[\alpha]_D^{25}$ +6.0 (*c* 0.15, H_2O)].

N-Alkylations of pyrrolidine amide 11

*Methyl N-butyl-2,5-dideoxy-2,5-imino-D-mannonamide **35**.* 10% Palladium on carbon (13 mg, 10 mol%) and butyraldehyde (0.024 mL, 0.26 mmol) were added to a solution of methyl 2,5-dideoxy-2,5-imino-D-mannonamide **11** (25 mg, 0.13 mmol) in a mixture of dioxane (0.5 mL) and water (0.5 mL). The reaction was purged with argon and then hydrogen and stirred under a hydrogen atmosphere for 18 h. After this time mass spectrometry indicated the loss of starting material ($[M + H]^+$, 191) and the formation of the alkylated iminosugar ($[M + H]^+$, 247). The reaction was purged with argon, filtered (glass microfiber) and concentrated *in vacuo*. The crude residue was purified by ion exchange chromatography (Dowex 50 W X8, H^+) to give the iminosugar **35** as a yellow oil (29 mg, 88%).

HRMS (ESI +ve): found 247.1657 ($[M + H]^+$); $C_{11}H_{23}N_2O_4$ requires: 247.1652; $[\alpha]_D^{25}$ −40.3 (*c*, 0.66 in MeOH); ν_{max} (thin film, Ge): 3333 (s, br, OH/NH), 1651 (s, amide I), 1545 (m, amide II); δ_H (400 MHz, D_2O): 0.87 (3H, t, Me, *J* 7.3), 1.22–1.36 (2H, m, $MeC\underline{H}_2$), 1.37–1.47 (2H, m, $MeCH_2C\underline{H}_2$), 2.57–2.70 (2H, m, $C\underline{H}_2N$), 2.77(3H, s, $NC\underline{H}_3$), 3.23 (1H, a-q, H5, *J* 4.2), 3.45 (1H, d, H2, *J* 3.8), 3.76 (1H, dd, H6, *J* 4.0, J_{gem} 12.4), 3.78 (1H, dd, H6′, *J* 5.0, 12.1), 3.99 (1H, a-t, H4, *J* 3.6), 4.03 (1H, a-t, H3, *J* 3.7); δ_C (100.6 MHz, D_2O): 13.8 ($\underline{C}H_3CH_2$), 20.6 ($Me\underline{C}H_2$), 26.1 ($N\underline{C}H_3$), 30.1 ($MeCH_2\underline{C}H_2$), 48.5 ($N\underline{C}H_2$), 59.6 (C6), 68.6 (C5), 72.9 (C2), 79.1 (C4), 80.7 (C3), 175.7 (C═O); *m*/*z* (ESI +ve): 515 ($[2M + H]^+$, 100%), 305 ($[M + MeCN + NH_4]^+$, 45%), 269 ($[M + Na]^+$, 40%), 247 ($[M + H]^+$, 35%).

*Methyl N-hydroxyethyl-2,5-dideoxy-2,5-imino-D-mannonamide **36**.* 10% palladium on carbon (15 mg, 10 mol%) and glycolaldehyde dimer (35 mg, 0.30 mmol) were added to a solution of methyl 2,5-dideoxy-2,5-imino-D-mannonamide **11** (28 mg, 0.15 mmol) in a mixture of dioxane (0.5 mL) and water (0.5 mL). The reaction was purged with argon and then hydrogen and stirred under a hydrogen atmosphere for 18 h. After this time mass spectrometry indicated the loss of starting material ($M + H^+$, 191) and the formation of the alkylated iminosugar ($M + H^+$, 235). The reaction was purged with argon, filtered (glass microfiber) and concentrated *in vacuo*. The crude residue was purified by ion exchange chromatography (Dowex 50 W X8, H^+) to give the iminosugar **36** as a yellow oil (32 mg, 93%).

HRMS (ESI +ve): found 235.1290 ($[M + H]^+$); $C_9H_{19}N_2O_5$ requires: 235.1288; $[\alpha]_D^{25}$ −24.0 (*c*, 0.77 in MeOH); ν_{max} (thin film, diamond ATR): 3292 (s, br, OH), 1638 (s, amide I), 1547 (m, amide II); δ_H (400 MHz, D_2O): 2.72–2.81 (1H, m, $C\underline{H}_2N$), 2.77 (3H, s, $NC\underline{H}_3$), 2.91–2.99 (1H, m, $C\underline{H}_2N$), 3.28–3.32 (1H, m, H5), 3.50 (1H, d, H2, $J_{2,3}$ 1.5), 3.59 (1H, dt, $CH_2C\underline{H}_2OH$, *J* 4.5, J_{gem} 11.2), 3.63–3.70 (1H, m, $CH_2C\underline{H}_2OH$), 3.77 (1H, dd, H6, $J_{6,5}$ 4.6, J_{gem} 12.5), 3.81 (1H, dd, H6′, $J_{6',5}$ 3.4, J_{gem} 12.5), 4.01–4.05 (2H, m, H3, H4); δ_C (125.6 MHz, D_2O): 26.2 ($N\underline{C}H_3$), 49.9 ($N\underline{C}H_2$), 59.5 (C6), 59.9 ($CH_2\underline{C}H_2OH$), 68.2 (C5), 73.2 (C2), 79.0, 80.7 (C4/C3), 175.9 (C═O); *m*/*z* (ESI +ve): 491 ($[2M + H]^+$, 18%), 257 ($[M + Na]^+$, 100%), 235 ($[M + H]^+$, 14%); *m*/*z* (ESI −ve): 503 ($[2M + Cl]^-$, 25%), 269 ($[M + Cl]^-$, 84%), 233 ($[M - H]^-$, 35%), 148 (100%).

*Methyl N′-[2-carboxyethyl]-2,5-dideoxy-2,5-imino-D-mannonamide **37**.* Methyl 2,5-dideoxy-2,5-imino-D-mannonamide **11** (11 mg, 0.06 mmol) was dissolved in a mixture of *tert*-butyl acrylate (0.5 mL) and methanol (1.5 mL). The mixture was stirred at 55 °C for 9–10 days, after which the reaction was judge to be complete by mass spectrometry. The mixture was reduced *in vacuo* to afford a pale yellow oil. This crude was re-dissolved in a mixture of trifluoroacetic acid (1.0 mL) and water (1.0 mL) and the resulting solution was stirred at rt. After 48 hours, the solvents were removed *in vacuo*. The remaining residue was loaded onto a Dowex 50 W X8, H^+ ion exchange resin. The column was flushed with water and then eluted with 2 M aqueous ammonia. The ammoniacal fraction was reduced *in vacuo* to afford iminosugar **37** as a yellow oil (15.1 mg, 99%).

HRMS (ESI −ve): found 261.1094 ($[M - H]^-$); $C_{10}H_{27}N_2O_6$ requires: 261.1092; $[\alpha]_D^{25}$ −28.4 (*c* 0.54, water); ν_{max} (thin film): 3247 (OH), 1641, 1564 (CO); δ_H (D_2O, 400 MHz): 2.48–2.53 (2H, m, $C\underline{H}_2COO$), 2.81 (3H, s, CH_3), 3.15–3.30 (2H, m, $C\underline{H}_2N$), 3.60 (1H, q, H5, $J_{5,6a} = J_{5,6b} = J_{5,4} = 4.0$), 3.82 (1H, d, H2, $J_{2,3}$ 4.4), 3.90 (1H, dd, H6, $J_{6,5}$ 4.0, J_{gem} 12.8), 3.95 (1H, dd, H6′, $J_{6',5}$ 4.4, J_{gem} 12.8), 4.12–4.14 (1H, m, H3), 4.16 (1H, t, H4, $J_{4,3} = J_{4,5}$ = 3.6); δ_C (D_2O, 100 MHz): 26.5 (CH_3), 33.8 ($\underline{C}H_2COO$), 46.3 ($\underline{C}H_2N$), 58.1 (C6), 69.2 (C5), 72.3 (C2), 77.8 (C4), 80.0 (C3), 171.7 (C1), 179.6 ($\underline{C}OO$); *m*/*z* (ESI^-): 261 ($[M - H]^-$, 100%), 523 ($[2M - H]^-$, 17%).

Biological experimental section[15a,39]

IC_{50} determinations. The enzymes β-*N*-acetylhexosaminidases (from human placenta, bovine kidney, jack bean, and *Aspergillus oryzae*), α-*N*-acetylgalactosaminidase (from chicken liver, *charonia lampas*) and *p*-nitrophenyl glycosides were purchased from Sigma-Aldrich Co. The cell lysate of human acute amyloid leukemia cell line HL-60 (RBRC) was used as the source of β-*N*-acetylhexosaminidase. For this purpose cells were cultured in RPMI 1640 medium containing 10% fetal calf serum, 100 units per mL of penicillin and 100 μg mL^{-1} streptomycin (Invitrogen) at 37 °C under 5% CO_2. On completion

cells were washed and centrifuged into a pellet from phosphate buffered saline. The cell pellet was then lysed in deionized H_2O (1.5 mL) using a glass dounce homogeniser and following centrifugation at 500*g* for 5 min at 4 °C, the supernatant was removed and used as enzyme source. The glycosidase activities were determined using an appropriate *p*-nitrophenyl glycoside as substrate at the optimum pH of each enzyme. The reaction mixture (1 mL) contained 2 mM of the substrate and the appropriate amount of enzyme. The reaction was stopped by adding 2 mL of 400 mM Na_2CO_3. The released *p*-nitrophenol was measured spectrometrically at 400 nm.

K_i measurements. For β-*N*-acetylhexosaminidase activity derived from HL-60 cells, cell homogenate was used in combination with 4-methylumbelliferyl-*N*-acetyl-β-D-glucosaminide (Sigma-Aldrich Co) as substrate. Method: enzyme (5 μL) and inhibitor solution (5 μL) were added to a 96-well microtitre plate which was pre-incubated at 37 °C for 5 min before starting the reaction by addition of 40 μL of the substrate solution. After a further 40 min of incubation at 37 °C the reaction was quenched by the addition of 200 μL of 0.5 M sodium carbonate (aq.). For HL-60 derived enzyme fluorescence was measured using a microtitre plate reader (Molecular Devices SPECTRAmax M5 Rom v2.1.35, Ex. 355 nm, Em. 460 nm, Cutoff 455 nm). Data sets in triplicate were subjected in Prism 4.0a to a Lineweaver–Burk analysis (1/rate against 1/[substrate concentration]) using a suitable range of substrate solutions (4, 2, 1, 0.75, 0.5, 0.2 mM) and inhibitor concentrations. The obtained slopes were plotted against the inhibitor concentration and the K_i obtained from the *X*-axis intercept. The corresponding Lineweaver–Burk plots can be found in the ESI.†

Free oligosaccharide analysis (FOS)

Materials. Sodium cyanoborohydride, bicinchoninic acid/copper(II) sulfate reagent, sodium acetate trihydrate and anthranilic acid (2-AA) from Sigma-Aldrich (Dorset, U.K.). Water was Milli-Q™ grade. Acetonitrile HPLC grade from Merk (Darmstadt, Germany), boric acid from BDH and Methanol from VWR (Lutterworth, Leicestershire, U.K.), ion exchange resins AG50-X12 and AG4-X4 from Biorad (Hemel Hampstead, Hertfordshire, U.K.), Speed amide 2 from Applied Separations (Allentown, Pennsylvania, U.S.), Amicon Ultra centrifugal filter from Millipore (Croxley, Watford, U.K.).

Inhibition treatment of HL60 cells and FOS isolation. The protocol was adapted from a literature procedure.[26] Having been propagated at a higher density, HL60 cells were seeded in a 6 well plate at a 5×10^5 cells per mL concentration and treated with 2 mL of fresh medium containing the pyrrolidine **11** or one of its derivatives **35**, **36**, **37**. HL60 cells were treated at concentrations of 200 μM, 50 μM and 5 μM for 24 h. DGJNAc **5** (500 μM) served as a positive control. Following incubation, cells were centrifuged at 350 g, 10 °C, for 7 min and the pellet was washed three times with PBS (5 mL). Washed cell pellets were stored at −20 °C until use. Following thawing at rt, samples were resuspended in 650 μL of water and Dounce homogenized. An aliquot of 50 μL was removed and treated for 16 h at rt with 2.6 μL NaOH (5 M) solution prior to protein concentration determination in comparison to a standard using bicinchoninic acid/copper(II) sulfate reagent (Sigma Aldrich). For desalting and deproteination, 500 μL of the homogenate was subjected to a mixed-bed ion-exchange column [0.2 mL of AG50-X12, (H^+, 100–200 mesh) 0.4 mL of AG4-X4, (OH^-, 100–200 mesh)], which had been preequilibrated with water (5 × 1 mL). The homogenate was added to the column and eluted with water (4 × 1 mL). The eluent containing the free oligosaccharides (FOS) was collected and dried by lyophilisation.

FOS fluorescent labeling. 2-AA labelling buffer was made as previously described:[40] Anthranilic acid (2-AA) was dissolved at 30 mg mL^{-1} in a solution containing 4% sodium acetate trihydrate (w/v) and 2% boric acid (w/v) in methanol. To this mixture sodium cyanoborohydride was added to a final concentration of 45 mg mL^{-1}.

The lyophilised samples were resuspended in 300 μL total of water, transferred to an Eppendorf tube and evaporated to dryness using a Thermo Savant (SPD121P) SpeedVac system. The dried samples were dissolved in 30 μL of water and 80 μL of 2-AA labeling buffer was added followed by incubation at 80 °C for 1 h.

Purification of the labeled FOS. After cooling, 1 mL of acetonitrile/water 97 : 3 was added to the labeled FOS samples, vortexed and added to a Spe-ed amide-2 column, which had been prewashed sequentially with 1 mL acetonitrile, 2 mL water and 2 mL acetonitrile. The column was washed with 2 mL of acetonitrile/water 95 : 5 and the 2-AA labeled FOS were eluted with water (2 × 0.75 mL) by gravity. Samples were stored at −20 °C until analysed by HPLC.

Carbohydrate analysis by normal phase HPLC. The Chromatography system used consisted of a Water Alliance 2695 separations module and an in-line Waters 474 fluorescence detector set at Exλ 360 nm and Emλ 425 nm.[41] The gain for the detector was set to 1000 and the emission bandwidth to 40 nm. Chromatography was performed at 30 °C. Solvent A was acetonitrile. Solvent B was water. Solvent C consisted of 800 mM ammonium hydroxide, titrated to pH 3.85 with acetic acid in water and was prepared using a standard ammonium hydroxide solution (5 M, Sigma Aldrich). Data collection and processing was performed using Waters Empower software. Glucose units were derived by comparison to a 2-AA labelled glucose oligomer ladder (obtained by partial digestion of dextran) as external standard. 50 μL of a 1 : 1 mixture sample/acetonitrile were injected for each run. Separation was performed on a 4.6 × 250 mm TSK gel-Amide 80 column (5 μM) (Anachem, Luton, Beds, U.K.) and the following gradient conditions were used for the analysis of the FOS samples: time = 0 min (t = 0), 71.6% A, 25.9% B, 2.5% C (0.8 mL min^{-1}); t = 6, 71.6% A, 25.9% B, 2.5% C (0.8 mL min^{-1}); t = 45, 46.2% A, 51.3% B, 2.5% C (0.8 mL min^{-1}); t = 46, 35% A, 62.5% B, 2.5% C (0.8 mL min^{-1}); t = 48, 35% A, 62.5% B, 2.5% C (0.8 mL min^{-1}); t = 49, 71.6% A, 25.9% B, 2.5% C (0.8 mL min^{-1}); t = 51, 71.6% A, 25.9% B, 2.5% C (1.2 mL min^{-1}); t = 64, 71.6% A, 25.9% B, 2.5% C (1.2 mL min^{-1}); t = 65, 71.6% A,

25.9% B, 2.5% C (0.8 mL min^{-1}). Labeled FOS glycans were assigned according to literature GUs[37] for known species, which had been characterized using MALDI-TOF mass spectrometry.[42]

Enzyme digest of FOS (Jack Bean β-*N*-acetyl-hexosaminidase). Glycosidase digest using jack bean β-*N*-acetyl-hexosaminidase (10 μL of 6 U mL^{-1} in 50 mM citrate buffer pH 5.0 containing 1 mg mL^{-1} BSA and 0.02% sodium azide, purified in house) was performed on a representative sample (100 μL) of the complete FOS population from 500 μM DGJNAc **5** treated HL60 cells. After 16 h incubation at 37 °C, the enzyme digest was diluted with 90 μL of water. An Amicon Ultra centrifugal filter (Millipore, 10 000 MWCO) was pretreated with 150 μL of water and used to remove proteins following centrifugation at 13 000*g* for 15 min at 4 °C. The filter was washed with an additional 100 μL of water and the combined eluates were evaporated to dryness before being reconstituted in 100 μL of a 1 : 1 mixture of acetonitrile/water for HPLC analysis.

Statistical analysis of FOS analysis. Experiments were performed in triplicate. To test for significance the Prism 4.0a software was used to perform a Student *t*-test using a 99% confidence interval.

Cell metabolism and cytotoxicity assay

In order to test an inhibitor for the interference with cell metabolism and associated cellular toxicity the following protocol was adapted from the CellTiter 96® AQ_{ueous} Non-Radioactive Cell Proliferation Assay (Promega, Southampton, U.K.). The corresponding compound in a variety of increasing concentrations was incubated with the cell line to be tested for 24 or 72 h. 100 μL of the cell line to be tested contained in their growth medium were transferred into a 96-well plate, 20 μL of development solution was added to each well and the mixture incubated for 4 h at 37 °C and 5% CO_2 before absorbance of the newly formed formazan was measured at 490 nm (Molecular Devices SPECTRAmax M5 Rom v2.1.35). The development solution is made up of a 20 : 1 mixture of 3-(4,5-dimethylthiazol-2-yl)-5-(3-carboxymethoxyphenyl)-2-(4-sulfophenyl)-2*H*-tetrazolium (MTS) in PBS (pH 6.5, sterile filtered and stored at −20 °C protected from light) and phenazine methosulfate (PMS) in PBS (0.92 mg mL^{-1}, sterile filtered), which were combined immediately before usage. This method was employed to rule out cellular toxicity in the case of the FOS assay involving the pyrrolidine **11** and derivatives **35**, **36**, **37**. Cellular toxicity by pyrrolidine **11** for MDA-MB-231 cells involved in the cell invasion assay was tested at concentrations up 1 mM. Detailed toxicity data of all compounds can be found in the ESI.†

Cell invasion assay – Boyden chamber setup

3 day protocol of cell invasion. The protocol was adapted from the instructions for the QCM™ 24-Well cell invasion assay (Merk Millipore, Watford, U.K., ECM 554) and involved steps spread over 3 days. The following protocol used cells grown in a 225 cm^2 flask and employed 12 wells in total of a 24 well plate. Day 1: cells having been grown for 2–3 passages following thawing, were placed in starvation medium (FCS free, no trypsination at this stage) for 24 h. Day 2: following a visual inspection the cells were washed with PBS (30 mL) and incubated for 15 min with 9 mL of trypsin (Sigma Aldrich) at 37 °C and 5% CO_2. To the detached cells 15 mL of quenching medium (Bovine serum albumin 50 mg mL^{-1} in starvation medium; sterile filtered) was added and the cells were centrifuged into a pellet (300*g*, 5 min). The pellet was re-dissolved in quenching medium and the cell number adjusted accordingly. To allow for rehydration 300 μL of pre-warmed starvation medium containing drug or distilled water (sterile filtered) at the final concentration was added to the top insert and incubated for 15–30 min at rt. The solution in the insert was then aspirated and discarded. The prepared cell solution was adjusted to the final concentration using drug or distilled water and 250 μL were added to the corresponding top insert. With exception of the negative control, where FCS free media was used, all bottom inserts were made up to the final concentration with drug and distilled water in regular cell growth medium containing FCS (chemo-attractant) and 500 μl were added to the corresponding bottom well. The thus prepared plate was then incubated at 37 °C at 5% CO_2 for 24–64 h.[43] Day 3: the remaining wells on the 24-well plate were filled with 225 mL of pre-warmed cell detachment buffer (contained in kit). The well insert was lifted up and the cell solution contained was carefully aspirated and discarded and the insert with the invaded cells attached to the bottom was placed in the well containing detachment buffer. Following the transfer of all the inserts to the new wells the plate was incubated for 30 min at 37 °C and gently shaken every 10 min. The inserts were then discarded and 75 μL of CyQUANT dye/lysis buffer (1 : 75 mixture of dye/lysis buffer)[44] was added to each well and the resulting solution incubated at rt for 15 min. Of the resultant solution 200 μL were transferred into a 96 well plate and fluorescence was determined (Molecular Devices SPECTRAmax M5 Rom v2.1.35, excitation 485 nm, emission 538 nm).

Statistical analysis. Experiments were performed in triplicate whenever possible and otherwise in duplicate. To test for significance the Prism 4.0a software was used to perform a Student *t*-test using a 95% confidence interval.

Protein concentration determination. Protein concentrations were determined as follows: in a 50 : 1 ratio bicinchoninic acid solution (Sigma-Aldrich, B9643) was combined with copper(II) sulfate solution (Sigma-Aldrich, C2284) and 200 μL of this solution was added to a 10 μL protein sample in a 96-well plate. Following incubation at 37 °C for 30 min absorbance was measured at 600 nm (Molecular Devices UVmax kinetic microplate reader and SOFTmax 2.35 software). Protein content in triplicate was determined in comparison to a protein standard (bovine serum albumin, Sigma-Aldrich, P0914).

Computational experimental section

DFT calculations at the M06-2X/6-311++G** level of theory using Gaussian 09 were performed to evaluate the optimized

geometries of **10**, **11**, **12**, **13**, **21**, **38** and **42** in gas phase.[45] Structures were rendered and overlayed as indicated in the corresponding figure description using the Maestro 9.3.5 software of the Schrödinger Suite 2012.

Acknowledgements

This work was supported by Cancer Research UK and an Oxford Glycobiology Scholarship (AFGG), Newton Abraham Research Fund (BJA), Grant-in-Aid for Scientific Research (C) (No: 26460143) (AK) from the Japanese Society for the Promotion of Science (JSPS), and the Leverhulme Trust (GWJF). The Research & Technological Innovation and Supercomputing Center of Extramadura (CénitS) is gratefully acknowledged for permitting the use of the supercomputer LUSITANIA.

References

1 S. A. Springer and P. Gagneux, *J. Biol. Chem.*, 2013, **288**, 6904–6911.
2 (*a*) K. Sandhoff and K. Harzer, *J. Neurosci.*, 2013, **33**, 10195–10208; (*b*) R. J. Desnick and A. M. Wang, *J. Inherited Metab. Dis.*, 1990, **13**, 549–559.
3 (*a*) J. S. S. Rountree, T. D. Butters, M. R. Wormald, S. D. Boomkamp, R. A. Dwek, N. Asano, K. Ikeda, E. L. Evinson, R. J. Nash and G. W. J. Fleet, *ChemMedChem*, 2009, **4**, 378–392; (*b*) M. B. Tropak, S. P. Reid, M. Guiral, S. G. Withers and D. Mahuran, *J. Biol. Chem.*, 2004, **279**, 13478–13487; (*c*) N. E. Clark, M. C. Metcalf, D. Best, G. W. J. Fleet and S. C. Garman, *Proc. Natl. Acad. Sci. U. S. A.*, 2012, **109**, 17400–17405; (*d*) P. Sears and C. H. Wong, *Angew. Chem., Int. Ed.*, 1999, **38**, 2300–2324.
4 (*a*) S. A. Yuzwa and D. J. Vocadlo, *Chem. Soc. Rev.*, 2014, **43**, 6839–6858; (*b*) N. Cekic, J. E. Heinonen, K. A. Stubbs, C. Roth, Y. He, A. J. Bennet, E. J. McEachern, G. J. Davies and D. J. Vocadlo, *Chem. Sci.*, 2016, **7**, 3742–3750.
5 (*a*) J. Alonso, M. Schimpl and D. M. F. van Aalten, *J. Biol. Chem.*, 2014, **289**, 34433–34439; (*b*) F. V. Rao, H. C. Dorfmueller, F. Villa, M. Allwood, I. M. Eggleston and D. M. F. van Aalten, *EMBO J.*, 2006, **25**, 1569–1578.
6 (*a*) M. Niedbala, R. Madiyalakan, L. Matta, K. Crickar, M. Sharma and R. Bernacki, *Cancer Res.*, 1987, **47**, 4634–4641; (*b*) P. A. Jones and Y. A. De Clerck, *Cancer Metastasis Rev.*, 1982, **1**, 289–317.
7 (*a*) B. Woynarowska, H. Wikiel, M. Sharma, N. Carpenter, G. Fleet and R. Bernacki, *Anticancer Res.*, 1992, **12**, 161–166; (*b*) K. T. Ramessur, P. Greenwell, R. Nash and M. V. Dwek, *Br. J. Biomed. Sci.*, 2010, **67**, 189–196.
8 (*a*) H. Umezawa, T. Aoyagi, T. Komiyama, H. Morishima, M. Hamada and T. Takeuchi, *J. Antibiot.*, 1974, **27**, 963–969; (*b*) T. Kudo, Y. Nishimura, S. Kondo and T. Takeuchi, *J. Antibiot.*, 1992, **45**, 954–962; (*c*) Y. Nishimura, *J. Antibiot.*, 2009, **62**, 407–423.
9 (*a*) H. Usuki, M. Toyo-oka, H. Kanzaki, T. Okuda and T. Nitoda, *Bioorg. Med. Chem.*, 2009, **17**, 7248–7253; (*b*) J.-S. Zhu, S. Nakagawa, W. Chen, I. Adachi, Y.-M. Jia, X.-G. Hu, G. W. J. Fleet, F. X. Wilson, T. Nitoda, G. Horne, R. van Well, A. Kato and C.-Y. Yu, *J. Org. Chem.*, 2013, **78**, 10298–10309.
10 (*a*) T. Aoyama, H. Naganawa, H. Suda, K. Uotani, T. Aoyagi and T. Takeuchi, *J. Antibiot.*, 1992, **45**, 1557–1558; (*b*) K. Tatsuta, S. Miura and H. Gunji, *Bull. Chem. Soc.*, 1997, **70**, 427–436.
11 (*a*) G. W. J. Fleet, L. E. Fellows and P. W. Smith, *Tetrahedron*, 1987, **43**, 979; (*b*) G. W. J. Fleet, P. W. Smith, R. J. Nash, L. E. Fellows, R. B. Parekh and T. W. Rademacher, *Chem. Lett.*, 1986, 1051.
12 (*a*) D. Best, C. Wang, A. C. Weymouth-Wilson, R. A. Clarkson, F. X. Wilson, R. J. Nash, S. Miyauchi, A. Kato and G. W. J. Fleet, *Tetrahedron: Asymmetry*, 2010, **21**, 311–319; (*b*) A. F. G. Glawar, D. Best, B. Ayers, S. Miyauchi, S. Nakagawa, M. Aguilar-Moncayo, J. M. García Fernández, C. O. Mellet, E. V. Crabtree, T. D. Butters, F. X. Wilson, A. Kato and G. W. J. Fleet, *Chem. – Eur. J.*, 2012, **18**, 9341–9359.
13 (*a*) E.-L. Tsou, Y.-T. Yeh, P.-H. Liang and W.-C. Cheng, *Tetrahedron*, 2009, **65**, 93–100; (*b*) J. Liu, M. M. D. Numa, H. Liu, S. J. Huang, P. Sears, A. R. Shikhman and C.-H. Wong, *J. Org. Chem.*, 2004, **69**, 6273–6283.
14 J. S. S. Rountree, T. D. Butters, M. R. Wormald, R. A. Dwek, N. Asano, K. Ikeda, E. L. Evinson, R. J. Nash and G. W. J. Fleet, *Tetrahedron Lett.*, 2007, **48**, 4287–4291.
15 (*a*) E. V. Crabtree, R. F. Martínez, S. Nakagawa, I. Adachi, T. D. Butters, A. Kato, G. W. J. Fleet and A. F. G. Glawar, *Org. Biomol. Chem.*, 2014, **12**, 3932–3943; (*b*) D. Best, S. F. Jenkinson, D. J. Watkin, F. X. Wilson, R. J. Nash and G. W. J. Fleet, *Acta Crystallogr.,Sect. E: Struct. Rep. Online*, 2009, **65**, o2418–o2419.
16 B. J. Ayers, A. F. G. Glawar, R. F. Martínez, N. Ngo, Z. Liu, G. W. J. Fleet, T. D. Butters, R. J. Nash, C.-Y. Yu, M. R. Wormald, S. Nakagawa, I. Adachi, A. Kato and S. F. Jenkinson, *J. Org. Chem.*, 2014, **79**, 3398–3409.
17 J. P. Shilvock, R. J. Nash, J. D. Lloyd, A. L. Winters, N. Asano and G. W. J. Fleet, *Tetrahedron: Asymmetry*, 1998, **9**, 3505–3516.
18 A. F. G. Glawar, S. F. Jenkinson, A. L. Thompson, S. Nakagawa, A. Kato, T. D. Butters and G. W. J. Fleet, *ChemMedChem*, 2013, **8**, 658–666.
19 (*a*) B. L. Mark, D. J. Mahuran, M. M. Cherney, D. Zhao, S. Knapp and M. N. G. James, *J. Mol. Biol.*, 2003, **327**, 1093–1109; (*b*) M. J. Lemieux, B. L. Mark, M. M. Cherney, S. G. Withers, D. J. Mahuran and M. N. G. James, *J. Mol. Biol.*, 2006, **359**, 913–929.
20 (*a*) A. F. G. Glawar, S. F. Jenkinson, S. J. Newberry, A. L. Thompson, S. Nakagawa, A. Yoshihara, K. Akimitsu, K. Izumori, T. D. Butters, A. Kato and G. W. J. Fleet, *Org. Biomol. Chem.*, 2013, **11**, 6886–6899; (*b*) G. M. J. Lenagh-Snow, S. F. Jenkinson, S. J. Newberry, A. Kato, S. Nakagawa, I. Adachi, M. R. Wormald, A. Yoshihara, K. Morimoto,

K. Akimitsu, K. Izumori and G. W. J. Fleet, *Org. Lett.*, 2012, **14**, 2050–2053.

21 G. W. J. Fleet, I. Bruce, A. Girdhar, M. Haraldsson, J. M. Peach and D. J. Watkin, *Tetrahedron*, 1990, **46**, 19–32.

22 I. Bruce, G. W. J. Fleet, I. Cenci di Bello and B. Winchester, *Tetrahedron*, 1992, **48**, 10191–10200.

23 (*a*) Y. Wang, G. W. J. Fleet, F. X. Wilson, R. Storer, P. L. Myers, C. J. Wallis, O. Doherty, D. J. Watkin, K. Vogt, D. R. Witty and J. M. Peach, *Tetrahedron: Asymmetry*, 1990, **1**, 527; (*b*) T. M. Krulle, B. Davis, H. Ardron, D. D. Long, N. A. Hindle, C. Smith, D. Brown, A. L. Lane, D. J. Watkin, D. G. Marquess and G. W. J. Fleet, *Chem. Commun.*, 1996, 1271–1272.

24 A. C. de S. Pereira, M. A. C. Kaplan, J. G. S. Maia, O. R. Gottlieb, R. J. Nash, G. Fleet, L. Pearce, D. J. Watkin and A. M. Scofield, *Tetrahedron*, 1991, **47**, 5637–5640.

25 J. Liu, A. R. Shikhman, M. K. Lotz and C. H. Wong, *Chem. Biol.*, 2001, **8**, 701–711.

26 S. D. Boomkamp, J. S. S. Rountree, D. C. A. Neville, R. A. Dwek, G. W. J. Fleet and T. D. Butters, *Glycoconjugate J.*, 2010, **27**, 297–308.

27 (*a*) Y. Zhao and D. G. Truhlar, *Theor. Chem. Acc.*, 2008, **120**, 215–241; (*b*) Y. Zhao and D. G. Truhlar, *Acc. Chem. Res.*, 2008, **41**, 157–167.

28 (*a*) A. D. Becke, *J. Chem. Phys.*, 1993, **98**, 5648–5652; (*b*) C. Lee, W. Yang and R. G. Parr, *Phys. Rev. B: Condens. Matter*, 1988, **37**, 785–789; (*c*) P. J. Stephens, F. J. Devlin, C. F. Chabalowski and M. J. Frisch, *J. Phys. Chem.*, 1994, **98**, 11623–11627.

29 N. Araújo, S. F. Jenkinson, R. F. Martínez, A. F. G. Glawar, M. R. Wormald, T. D. Butters, S. Nakagawa, I. Adachi, A. Kato, A. Yoshihara, K. Akimitsu, K. Izumori and G. W. J. Fleet, *Org. Lett.*, 2012, **14**, 4174–4177.

30 (*a*) G. M. J. Lenagh-Snow, N. Araujo, S. F. Jenkinson, R. F. Martinez, Y. Shimada, C.-Y. Yu, A. Kato and G. W. J. Fleet, *Org. Lett.*, 2012, **14**, 2142–2145; (*b*) G. M. J. Lenagh-Snow, N. Araujo, S. F. Jenkinson, C. Rutherford, S. Nakagawa, A. Kato, C.-Y. Yu, A. C. Weymouth-Wilson and G. W. J. Fleet, *Org. Lett.*, 2011, **13**, 5834–5837.

31 R. F. Martínez and G. W. J. Fleet, *Tetrahedron: Asymmetry*, 2014, **25**, 373–380.

32 H. B. Bosmann and R. J. Bernacki, *Exp. Cell Res.*, 1970, **61**, 379–386.

33 (*a*) B. Woynarowska, H. Wikiel and R. Bernacki, *Cancer Res.*, 1989, **49**, 5598–5604.

34 Merck Millipore: User guide for QCM 24-well cell invasion assay. http://www.millipore.com/userguides.nsf/a73664f9f981af8c852569b9005b4eee/860c5f3ae955a8068525790d0054127f/$FILE/ECM554.pdf.

35 R. M. Neve, K. Chin, J. Fridlyand, J. Yeh, F. L. Baehner, T. Fevr, L. Clark, N. Bayani, J.-P. Coppe, F. Tong, T. Speed, P. T. Spellman, S. DeVries, A. Lapuk, N. J. Wang, W.-L. Kuo, J. L. Stilwell, D. Pinkel, D. G. Albertson, F. M. Waldman, F. McCormick, R. B. Dickson, M. D. Johnson, M. Lippman, S. Ethier, A. Gazdar and J. W. Gray, *Cancer Cell*, 2006, **10**, 515–527.

36 (*a*) A. W. Millar, P. D. Brown, J. Moore, W. A. Galloway, A. G. Cornish, T. J. Lenehan and K. P. Lynch, *Br. J. Clin. Pharmacol.*, 1998, **45**, 21–26; (*b*) J. D. Evans, A. Stark, C. D. Johnson, F. Daniel, J. Carmichael, J. Buckels, C. W. Imrie, P. Brown and J. P. Neoptolemos, *Br. J. Cancer*, 2001, **85**, 1865–1870; (*c*) J. A. Sparano, P. Bernardo, P. Stephenson, W. J. Gradishar, J. N. Ingle, S. Zucker and N. E. Davidson, *J. Clin. Oncol.*, 2004, **22**, 4683–4690; (*d*) L. Coussens, B. Fingleton and L. Matrisian, *Science*, 2002, **295**, 2387–2392.

37 H. E. Gottlieb, V. Koplyar and A. Nudelman, *J. Org. Chem.*, 1997, **62**, 7512–7515.

38 C. Falentin, D. Beaupere, G. Demailly and I. Stasik, *Tetrahedron*, 2008, **64**, 9989–9991.

39 B. Mercer, S. F. Jenkinson, R. J. Nash, S. Miyauchi, A. Kato and G. W. J. Fleet, *Tetrahedron: Asymmetry*, 2009, **20**, 2368–2373.

40 D. S. Alonzi, D. C. A. Neville, R. H. Lachmann, R. A. Dwek and T. D. Butters, *Biochem. J.*, 2008, **409**, 571–580.

41 D. Neville, V. Coquard, D. Priestman, D. te Vruchte, D. Sillence, R. Dwek, F. Platt and T. Butters, *Anal. Biochem.*, 2004, **331**, 275–282.

42 H. Mellor, D. Neville, D. Harvey, F. Platt, R. Dwek and T. Butters, *Biochem. J.*, 2004, **381**, 861–866.

43 (*a*) L. A. Repesh, *Invasion Metastasis*, 1989, **9**, 192–208; (*b*) A. Albini, Y. Iwamoto, H. K. Kleinman, G. R. Martin, S. A. Aaronson, J. M. Kozlowski and R. N. McEwan, *Cancer Res.*, 1987, **47**, 3239–3245.

44 L. J. Jones, M. Gray, S. T. Yue, R. P. Haugland and V. L. Singer, *J. Immunol. Methods*, 2001, **254**, 85–98.

45 (*a*) M. J. Frisch, G. W. Trucks, H. B. Schlegel, G. E. Robb, J. R. Cheeseman, G. Scalmani, V. Barone, B. Mennucci, G. A. Petersson, H. Nakatsuji, M. Caricato, X. Li, H. P. Hratchian, A. F. Izmaylov, J. Bloino, G. Zheng, J. L. Sonnerberg, M. Hada, M. Ehara, K. Toyota, R. Fukuda, J. Hasegawa, M. Ishida, T. Nakajima, Y. Honda, O. Kitao, H. Nakai, T. Vreven, J. J. A. Montgomery, J. E. Peralta, F. Ogliaro, M. Bearpark, J. J. Heyd, E. Brothers, K. N. Kudin, V. N. Staroverov, R. Kobayashi, J. Normand, K. Raghavachari, A. Rendell, J. C. Burant, S. S. Iyengar, J. Tomasi, M. Cossi, N. Rega, N. J. millam, M. Klene, J. E. Knox, J. B. Cross, V. Bakken, C. Adamo, J. Jaramillo, R. Gomperts, R. E. Stratmann, O. Yazyev, A. J. Austin, R. Cammi, C. Pomelli, J. W. Ochterski, R. L. Martin, K. Morokuma, V. G. Zakrzewski, G. A. Goth, P. Salvador, J. J. Dannenberg, S. Dapprich, A. D. Daniels, Ö. Farkas, J. B. Foresman, J. V. Ortiz, J. Cioslowski and D. J. Fox, *Gaussian 09, Revision C.01*, Gaussian, Inc., Wallingford, CT, 2010; (*b*) Full details are given in the ESI.†